# Elucidating the contribution of stroke-induced changes to neural stem and progenitor cells associated with a neuronal fate

Damian Chwastek

Thesis submitted to the University of Ottawa
in partial fulfillment of the requirements for the
Master of Science in Neuroscience

Department of Cellular and Molecular Medicine
Faculty of Medicine
University of Ottawa

## Abstract

Following stroke there is a robust increase in the proliferation of neural stem and progenitor cells (NSPCs) that ectopically migrate from the subventricular zone (SVZ) to surround the site of damage induced by stroke (infarct). Previous *in vivo* studies by our lab and others have shown that a majority of migrating NSPCs when labelled *prior* to stroke become astrocytes surrounding the infarct. In contrast, our lab has shown that the majority of NSPCs when labelled *after* stroke become neurons surrounding the infarct. This thesis aims to elucidate the contributions of intrinsic changes that can alter the temporal fate of the NSPCs. The NSPCs were fate mapped in this study using the nestin-CreER$^{T2}$ mouse model and strokes were induced using the photothrombosis model within the cortex. In alignment with our previous findings, fate-mapping the NSPCs using a single injection of tamoxifen treatment revealed a temporal-specific switch in neuronal fate when NSPCs were labeled at timepoints greater than 7 days following stroke. Single cell RNA sequencing and histological analysis identified significant differences in the proportion of populations of NSPCs and their progeny labeled at the SVZ in the absence or presence of a stroke. NSPCs labelled *after* stroke were comprised of a reduced proportion of quiescent neural stem cells alongside an accompanied increase in doublecortin-expressing neuroblasts. The RNA transcriptional profile of the NSPCs labelled also revealed NSPCs and their progeny labeled *after* stroke had an overall enrichment for a neuronal transcription profile in all of the labeled cells with a reduction in astrocytic gene expression in quiescent and activated neural stem cells. Furthermore, we highlight the presence of perturbed transcriptional dynamics of neuronal genes, such as doublecortin following stroke. Altogether, our study reveals following a stroke there is a sustained intrinsic regulated neuronal-fated response in the NSPCs that reside

in the SVZ that may not be exclusive from extrinsic regulation. This work raises the challenge to learn how to harness the potential of this response to improve recovery following stroke through examining their contributions to recovery.

# *Table of Contents*

# List of Figures

## List of Abbreviations

| | |
|---|---|
| ACSF | Artificial cerebrospinal fluid |
| aNSCs | Activated neural stem cells |
| BDNF | Brain-derived neurotrophic factor |
| BrdU | Bromodeoxyuridine |
| CC | Corpus collosum |
| CCR2 | C-C chemokine receptor type 2 |
| CXCR4 | C-X-C chemokine receptor type 4 |
| DAPI | 4',6-diamidino-2-phenylindole |
| DCX | Doublecortin |
| eNBS | Early neuroblasts |
| FACS | Fluorescent activated cell sorting |
| fMRI | Functional Magnetic Resonance Imaging |
| GO | Gene ontology |
| lNBS | Late Neuroblasts |
| MCAO | Middle cerebral artery occlusion |
| MCP-1 | Monocyte chemoattractant protein-1 |
| MSNs | Medium spiny neurons |
| NBs | Neuroblasts |
| NES | Normalized enrichment score |
| NSCs | Neural stem cells |
| NSPCs | Neural stem and progenitor cells |
| Oligos | Oligodendrocytes |
| PBS | Phosphate buffered saline |
| PCR | Polymerase chain reaction |
| PFA | Paraformaldehyde |
| qNSCs | Quiescent neural stem cells |
| SBR | Spontaneous biological recovery |

| | |
|---|---|
| scRNAseq | Single cell RNA sequencing |
| SDF-1 | Stromal cell-derived factor 1 |
| SEM | Standard error of the mean |
| SGZ | Subgranular zone |
| SRF | Serum response factor |
| SVZ | Subventricular zone |
| TAM | Tamoxifen |
| TAPs | Transit amplifying progenitors |
| TF | Transcription factor |
| Thbs4 | Thrombospondin 4 |
| TNFR-1 | Tumor necrosis factor receptor 1 |
| UMAP | Uniform manifold approximation and projection |
| VEGF | Vascular endothelial growth factor |
| WT | Wild-type |

## Acknowledgements

When I came into the lab on my first day as an MSc candidate, I would have never expected the whirlwind of a ride completing this thesis would have been. From performing tons of exciting experiments to attending countless thought-provoking talks, from enduring a pandemic to surviving an atrocious bike crash, this journey has been quite the roller coaster for myself. In the end I made it, and for that I have many to thank for joining me on this ride.

To my supervisor Diane, I would like to thank you for taking me into your lab and providing me with countless opportunities and supporting me in defining my own path. Because of you I have learned the need to stand behind myself and not waiver in my beliefs, alongside finding the resilience that was necessary to complete this thesis and harness this resilience in my future endeavours.

To my family, my postsecondary education has tested me in countless ways, and you have been there throughout this chapter of my life. Because of you I have learned to find strength in myself and the confidence to stand on my own.

To my lab members, past and present, I thank you for being there to contribute to thoughtful conversations regarding our work and helping me with experiments as needed. Yingben, you are the one lab member present from start to finish of my time in the lab and an unquestionable source of support and I truly wish you all the best in the future.

To my friends, I would like to thank you for being pillars of unwavering support along this journey. Sarah, Sebastian, Candice, Nate, Nima, and Zanna: as fellow trainees and friends you have been there as sources of joy and torment in the best possible ways and brought numerous highs to this ride. Tyler and Claire: as roommates and friends you have endured my antics and

fostered a home for me to escape to, accepting and supporting me as I am throughout our time together. Caroline, Joey, Karol, Maia and Han: as my closest friends and my pandemic pod you never let me lose the joy and have been here championing me throughout this journey. I find myself closing this chapter still being a bit lost, but more found than I have ever been and for that I thank you.

# 1. Introduction

## 1.1 Stroke Recovery

Stroke is the leading cause of long-term disability in Canada with over 400,000 Canadians living with stroke-induced long-term disabilities (Wein et al., 2018). Research has led to new treatments to increase the survival of patients following stroke, yet there are no effective treatments to restore full recovery (Langhorne et al., 2011). Interestingly, during the early stages of recovery in both humans and animal models of stroke, partial recovery of function has been shown to occur in the absence of treatment (Cramer, 2008; Murphy and Corbett, 2009; Cassidy and Cramer, 2017). This endogenous phenomenon of recovery is known as spontaneous biological recovery (SBR). The need for enhanced treatments for stroke recovery has contributed to many labs, including our own, to focus on research aimed at understanding the effects of stroke on the adult brain and the endogenous recovery mechanisms that occur during SBR.

Previous studies have identified multiple endogenous mechanisms supporting SBR, such as angiogenesis, cortical reorganization and neurogenesis. Angiogenesis, the process of forming new blood vessels, has been shown to occur in the peri-infarct region of stroke patients (Ergul et al., 2012). In animal models of stroke, increased angiogenesis correlates with improved recovery, while inhibition of post-stroke angiogenesis correlates with reduced post-stroke recovery (Gertz et al., 2006). In addition, cortical reorganization has been observed in human patients following stroke. For example, using functional magnetic resonance imaging (fMRI), increases in neural activity bilaterally during the early stages following stroke alongside increased activity in the contralesional hemisphere being associated with reduced recovery following stroke was shown

to occur (Grefkes and Ward, 2014). Alongside angiogenesis and cortical reorganization, in 2006 adult neurogenesis was first described and hypothesized to be involved in SBR following stroke (Thored et al., 2006)

**1.2 Adult Neurogenesis**

Adult neurogenesis is a process that culminates in the generation of new neurons from neural stem and progenitor cells (NSPCs) in the adult mammalian brain (Miller and Gauthier-Fisher, 2009). The presence of NSPCs has been observed in many adult non-human mammals in both the subgranular zone (SGZ) of the hippocampus and the subventricular zone (SVZ) of the lateral ventricles. However it has been debated about whether neurogenesis occurs in these regions in adult humans (Bergmann et al., 2015). Initial evidence of neurogenesis persisting through adulthood in humans came from a study showing the presence of bromodeoxyuridine (BrdU) in hippocampal neurons, indicative of the presence of newly generated neurons in the adult brain (Eriksson et al., 1998). Debate about the validity of such findings comes from this study, and others that have examined post-mortem human tissue from patients with various neurological disorders, which likely has contributed to the conflicting findings (Boldrini et al., 2018; Kempermann et al., 2018; Sorrells et al., 2018). This limitation was overcome in a recent study that used tightly controlled conditions for isolating and processing tissue samples and showed the presence of immature neurons through adulthood in humans (Moreno-Jiménez et al., 2019). Thus these most recent findings strongly suggest that neurogenesis persists throughout adulthood in humans.

Adult neurogenesis is maintained through adulthood by NSPCs which have the ability to divide and form adult-generated neurons. Within the SVZ, there are three primary cell types that

contribute to adult neurogenesis: the Type B neural stem cells (NSCs); the Type C transit-amplifying progenitor cells (TAPs), and the Type A neuroblast cells (NBs) (Lim and Alvarez-Buylla, 2016). These cells are found in various domains of the SVZ: the apical domain which contains apical processes of NSCs; the intermediate domain which contains the NSCs that make contact with PCs and NBs; and the basal domain where basal processes of NSCs are in contact with blood vessels (Lim and Alvarez-Buylla, 2016). This organization of the subventricular zone thus allows for the lifelong activity of adult NSCs and the continuous generation of adult-born neurons through adulthood.

The discovery of adult NSPCs was first based on *in vitro* experiments using cells isolated from the SVZ that had the ability to self-renew and were multipotent when cultured with high concentrations of growth factors (Bond et al., 2015). *In vivo,* NSPCs from the SVZ primarily become olfactory bulb interneurons or oligodendrocytes within the corpus callosum (CC) (Rousselot et al., 1995; Menn et al., 2006). Additionally, the fate of NSPCs is further specified, in part, by their location within the SVZ and wall of the lateral ventricle. For example, ventral NSCs have been shown to often take up a calbindin-expressing periglomerular fate, whereas dorsal NSCs can be seen to take up a superficial granular fate (Merkle et al., 2007). Within the olfactory bulb adult-born neurons have been shown to be essential for proper olfactory function, which includes predator avoidance and odor discrimination (Sakamoto et al., 2011; Li et al., 2018).

There have been many significant recent developments in the field of adult neurogenesis due to the establishment of single cell RNA sequencing (scRNAseq), which allows for characterizing the transcriptional profile of cells at a single cell level. scRNAseq has been successfully used to characterize the NSPC populations residing in the SVZ of naïve mice (Llorens-

Bobadilla et al., 2015; Morizur et al., 2018; Shah et al., 2018; Zywitza et al., 2018). This new data suggests that quiescent neural stem cells (qNSCs) can be divided into dormant or primed for activation, and the activated neural stem cells (aNSCs) can be divided into active or transitioning to actively dividing. Such studies also identified a variety of markers that can be used as tools in histology and genetic targeting to differentiate between these populations. For example, primed qNSCs can be distinguished from dormant qNSCs based on high expression of Thbs4 and low levels of Vcam1, while dormant qNSCs highly express Slc1a3 and Troy (Basak et al., 2018). Together these findings highlight the strength of scRNAseq to characterize the regulatory mechanisms and profiles of NSPCs and their dynamic balance between poised potential and active restraint.

**1.3 Stroke & Adult Neurogenesis**

Following stroke there are many significant changes occurring involving NSPCs in the SVZ, which involves cellular and molecular programs that together drive changes in NSPC proliferation, differentiation and migration. The following sections will provide an extensive review of stroke-induced changes in neurogenesis.

**1.3a Stroke-Induced Changes Supporting NSPC Proliferation**

Following stroke there is a large disruption to the behavior of resident NSPCs found within the SVZ. Specifically, many studies have shown a striking increase in proliferation of NSPCs within the SVZ that peaks between one to two weeks post-stroke (Marlier et al., 2015). The combined increase in proliferation and ectopic migration of NSPCs post-stroke have been shown in many

preclinical models using the thymidine analog BrdU, as well as transgenic mouse models and viral strategies to label the dividing cells (Arvidsson et al., 2002; Zhang et al., 2004; Faiz et al., 2015).

Numerous mechanisms have been implicated in the increased NSPC proliferation observed to occur following stroke. For example, microRNAs, including miR-124a and miR17-92, are such targets that underlie changes in proliferation of NSPCs (Liu et al., 2011; Liu et al., 2013). miR17-92 has been shown to be overexpressed in the SVZ via the sonic hedgehog signaling pathway that is stimulated following stroke (Liu et al., 2013). Corresponding to such changes, targeted inhibition of miR17-92 following stroke leads to reduced cell proliferation post-stroke. Alongside increased levels of sonic hedgehog, increases in its upstream regulator Notch1 have been shown to occur (Wang et al., 2009). In response to such increases, targeting Notch1 by inhibition of the signaling pathway is shown to reduce stroke-induced NSPC proliferation (Wang et al., 2009).

Furthermore, a part of the stroke-induced immune response in the form of increased microglia numbers is shown to contribute to elevated NSPC proliferation. Specifically, in tandem with increased microglia numbers following stroke, there are increases in tumor necrosis factor receptor 1 (TNFR-1) expression at the SVZ, with mice lacking TNFR-1 having enhanced NSPC proliferation following stroke (Iosif et al., 2008). Such regulation by TNFR-1 indicates that there is both positive and negative regulation of NSPC proliferation occurring post stroke (Iosif et al., 2008). Together, these findings highlight a multitude of changes occurring at the level of the stroke SVZ that are both sufficient to induce and regulate the rate of proliferation of NSPCs, with the specific stroke-derived contributions to these mechanisms remaining to be determined.

Work by Llorens-Bobadilla et al. (2015) investigated changes in lineage-specific transcription factors in SVZ-derived NSPCs, in an attempt to characterize the molecular hallmarks of state transitions both under homeostasis and after injury. This study was performed using scRNAseq to characterize differences in SVZ-derived NSPCs after induction of ischemic striatal damage by use of a transient bilateral common carotid artery occlusion. Following injury, they show NSPCs transition into an activated state, which is accompanied by the activation of protein synthesis and cell cycle genes within the heterogeneous classes of cells within the NSPC lineage. Further, they identified an injury-induced overrepresentation of interferon gamma target genes underlying changes in the transcriptional profile of NSPCs following injury, with triggering of interferon signaling underlying the changes observed in NSPC transition. Given these and previous findings reviewed, it can be well appreciated the extent to which stroke induces activation of NSPCs to proliferate and form new cells.

Although stroke-induced proliferation in the SVZ has been shown in humans by use of birth dating cells in the SVZ, it is not well established to what degree stroke-induced migration of NSPCs is conserved in humans (Jin et al., 2006; Macas et al., 2006; Martí-Fàbregas et al., 2010). Jin et al. (2016) performed immunohistochemical staining for Ki67, a cell cycle marker (Sarli et al., 1994), on human brain biopsied sections and identified significant increases in the number of Ki67+ cells in the region adjacent to the infarct. They also showed the presence of doublecortin (DCX), a marker of immature neurons (Brown et al., 2003), in the ischemic penumbra. In agreement with this work, Macas et al. (2006) used post-mortem tissue and identified increases in the number of Ki67+ cells in the ipsilesional SVZ. In contrast, Huttner et al. (2014) by use of $^{14}C$ birth dating, which has been previously used to identify the presence of adult neurogenesis in

the naïve human brain, did not show any signs of stroke-induced neurogenesis in the adult brain. However, these contrasting findings between the immunohistological and $^{14}C$ studies could be due to many factors, including the relatively small amount of stroke-induced neurogenesis observed with age, high rate of death of cells once they migrate to the site of injury, and low sensitivity of $^{14}C$ birth dating. Together, these findings are suggestive of the presence of stroke-induced proliferation in humans, but the extent of the response remains to be determined.

**1.3b Stroke-Induced Changes in the Cortex Supporting NSPC Migration**

The increase in proliferation of NSPCs following stroke is accompanied by ectopic migration of the NSPCs out of the SVZ and towards the site of injury (Lindvall and Kokaia, 2015). The target area of ectopic migration is specific to the model and location of stroke, with NSPCs migrating to the cortex following focal cortical strokes, or migrating to the striatum following the striatum-damaging middle cerebral artery occlusion (MCAO) model (Arvidsson et al., 2002; Faiz et al., 2015). The observed proliferation and ectopic migration of SVZ-residing NSPCs is observed to begin as early as 3 days following stroke, with NSPCs observed migrating to the site of injury up to 16 weeks after injury (Thored et al., 2007; Faiz et al., 2015). Such changes in NSPC behavior are observed alongside long-term increases in the number of NSPCs in the SVZ, and thus highlight the presence of long-term changes to the SVZ microenvironment after stroke (Thored et al., 2006).

A key player underlying the migratory response derived from the SVZ to the site of injury is the reduction of oxygen at the site of stroke (Fisher, 2010). This is due to the interruption of blood flow caused by either blockage of blood vessels in the case of ischemic stroke, or rupturing of blood vessels in the case of hemorrhagic stroke (Fisher, 2010). Given the lack of adequate

oxygen supply, neurons face high levels of oxidative stress that ultimately leads to cell death (Kim et al., 2008). In response to cell death, the region of injury is observed to have its inflammatory response induced. This consists partly of increased reactivity of resident astrocytes alongside activation of microglia, in tandem with stroke-induced changes in the vasculature (Beck and Plate, 2009). As reviewed in the remainder of this section, changes that occur with the reactive astrocytes, microglia, as well as vasculature have been shown to contribute to stroke-induced NSPC migration.

Following transition to a reactive state, astrocytes secrete the chemokine stromal cell-derived factor (SDF-1) at the site of injury (Imitola et al., 2004). C-X-C chemokine receptor type 4 (CXCR4), a receptor for SDF-1, is expressed on SVZ-derived NSPCs, and thus contributes to the recruitment of SVZ-derived cells to the site of injury (Ji et al., 2004). Such recruitment has been established to occur, with overexpression of SDF-1 leading to enhanced NSPC recruitment, with blockade of the CXCR4 receptor leading to reduced NSPC recruitment. Furthermore, reactive astrocytes upregulate monocyte chemoattractant protein-1 (MCP-1) in the injured cortex and striatum (Yan et al., 2007). CCR type 2 (CCR2), the receptor for MCP-1, is also expressed in emigrating NBs, with knockout of either CCR2 or MCP-1 inducing reduced emigration of cells from the SVZ (Yan et al., 2007). Together, these findings highlight the impact of reactive astrocytes on supporting SVZ-derived migration of NSPCs.

Activated microglia also secrete chemoattractants that aid in the recruitment of NSPCs to the site of injury, such as vascular endothelial growth factor (VEGF) (Plate et al., 1999). This is observed from *in vitro* work showing VEGF acting as a chemoattractant, and *in vivo* work showing overexpression of VEGF increasing the number of recruited cells at the site of injury (Zhang et al.,

2003; Wang et al., 2007; Barkho et al., 2008). However, it remains unclear whether VEGF has specific effects on increasing migration independent of its ability to increase cell proliferation. Activated microglia also secrete the acidic glycoprotein osteopontin, another known chemoattractant (Meller et al., 2005). Following stroke, osteopontin induces neuroblast migration to the site of injury via the β1-integrin receptor expressed on SVZ-derived PCs (Yan et al., 2009). The need of osteopontin and β1-integrin for sufficient NSPC migration has been shown by blocking these targets contributing to inhibited cell migration (Yan et al., 2009). Thus, glial cells at the site of injury play a heavy role in the migration of SVZ-derived cells, with a multitude of chemokines and chemoattractants regulating migration to the site of injury.

The vasculature has been shown to be implicated in signaling supporting recruitment of NSPCs to the site of injury. The migration route taken up by NSPCs to the site of injury occurs through a synergistic relationship with the native microenvironment and neo-vasculature in the injured brain. Increased angiogenesis is observed in the injured cortex due to proliferation of endothelial cells occurring up to 3 weeks following stroke (Hayashi et al., 2003; Beck and Plate, 2009). These endothelial cells express Ang-1 , which is a target of Tie-2 receptors expressed on neuroblasts (Ohab et al., 2006), and thus contributing to the guidance of cells migrating to the site of injury. Furthermore, NBs have been shown to be in close proximity to blood vessels as they migrate from the SVZ, which has led to the suggestion that the blood vessels are being used as a substrate for migration by SVZ-derived cells (Thored et al., 2007; Kojima et al., 2010). Together these data make many strong positive links for the number of migrating cells increasing as the region of injury increases (Moraga et al., 2014), and thus the extent of recruitment mechanisms post-stroke appears to be due to in part by the extent of damage present.

**1.3c NSPC Fate Following Stroke**

Interestingly, the fate of NSPCs following stroke is quite different than what is seen under naïve conditions in the adult brain. As reviewed, numerous studies have examined the fate of cells following migration to the site of injury (Ohab and Carmichael, 2008; Lagace, 2012; Lindvall and Kokaia, 2015). There is a clear consensus in the field that following any type of stroke a majority of the cells die following migration (Arvidsson et al., 2002) and the large majority of cells that do survive following migration will take up an astrocyte phenotype (Benner et al., 2013). There is also recent work showing a significant proportion differentiate into reactive astrocytes within the core of the infarct (Faiz et al., 2015).

Although the majority of the cells have a glial fate surrounding the stroke, others have shown that a limited number of SVZ-derived NSPCs can also develop into neurons in the peri-infarct region *in vivo* (Zhang et al., 2004; Yamashita et al., 2006; Palma-Tortosa et al., 2017; Kannangara et al., 2018; Liang et al., 2019), with less than 1% of lost neurons being replaced by this endogenous response (Arvidsson et al., 2002). Work from our lab has also shown ~10% of cells in the peri-infarct region have a neuronal phenotype, as characterized by being able to fire action potentials (Kannangara et al., 2018). Similar to the NBs during development in the adult brain, the NBs in the peri-infarct region are hyper-excitable, receiving primarily GABAergic synaptic inputs, and have the capacity to integrate into the cortex. However, the limited number and sparse innervation likely limits their capacity to participate in recovery.

Surprisingly, additional work from our lab performed by Maheen Ceizar (PhD student), suggests that there are differences in the fate of NSPCs and their progeny relative to the timing of the labeling of NPSCs and induction of stroke (Ceizar, 2017). Given there is an increase in proliferation of NSPCs residing in the SVZ following stroke, Maheen performed fate-mapping of

NSPCs labelled both **before** or **after** photothrombotic stroke induction in an iBax mouse model (Sahay et al., 2011) and control wild-type (WT) littermates to determine if allowing more cells to survive following stroke would improve behavioral recovery post-stroke. As expected, in both the iBax and WT mice, fate-mapping of YFP-expressing NSPCs labeled with tamoxifen (TAM) before stroke revealed that the nestin+ NSPCs and their progeny primarily have an astrocytic fate in the peri-infarct region (Fig 1A-C; WT only shown). Specifically, in WT mice ~70% of the NSPC progeny at 12 weeks after labeling expressed the astrocytic marker GFAP, and <20% express the immature neuronal marker DCX. This finding is agreement with the majority of studies that have examined the fate and functional role of NSPCs after stroke and suggest that the majority of migrating cells become astrocytes. Surprisingly, in contrast, when the NSPCs were labeled with TAM after stroke, a majority of migrated NSPCs had a neuronal fate in both the iBax and WT mice (Fig 1D-F; WT only shown). Specifically, in WT mice less then 20% of the YFP+ NSPC progeny at 12 weeks post-stroke express GFAP and approximately 50% express DCX. These results were very interesting since they suggest that there are differences in the fate of NSPCs and their progeny relative to the timing of the labeling of NPSCs and induction of stroke. We hypothesize that others had not observed this neurogenic response after stroke, as they had labeled the NSPCs before stroke. This observation highlights that a lot remains unknown about the stroke-induced contributions to NSPC fate.

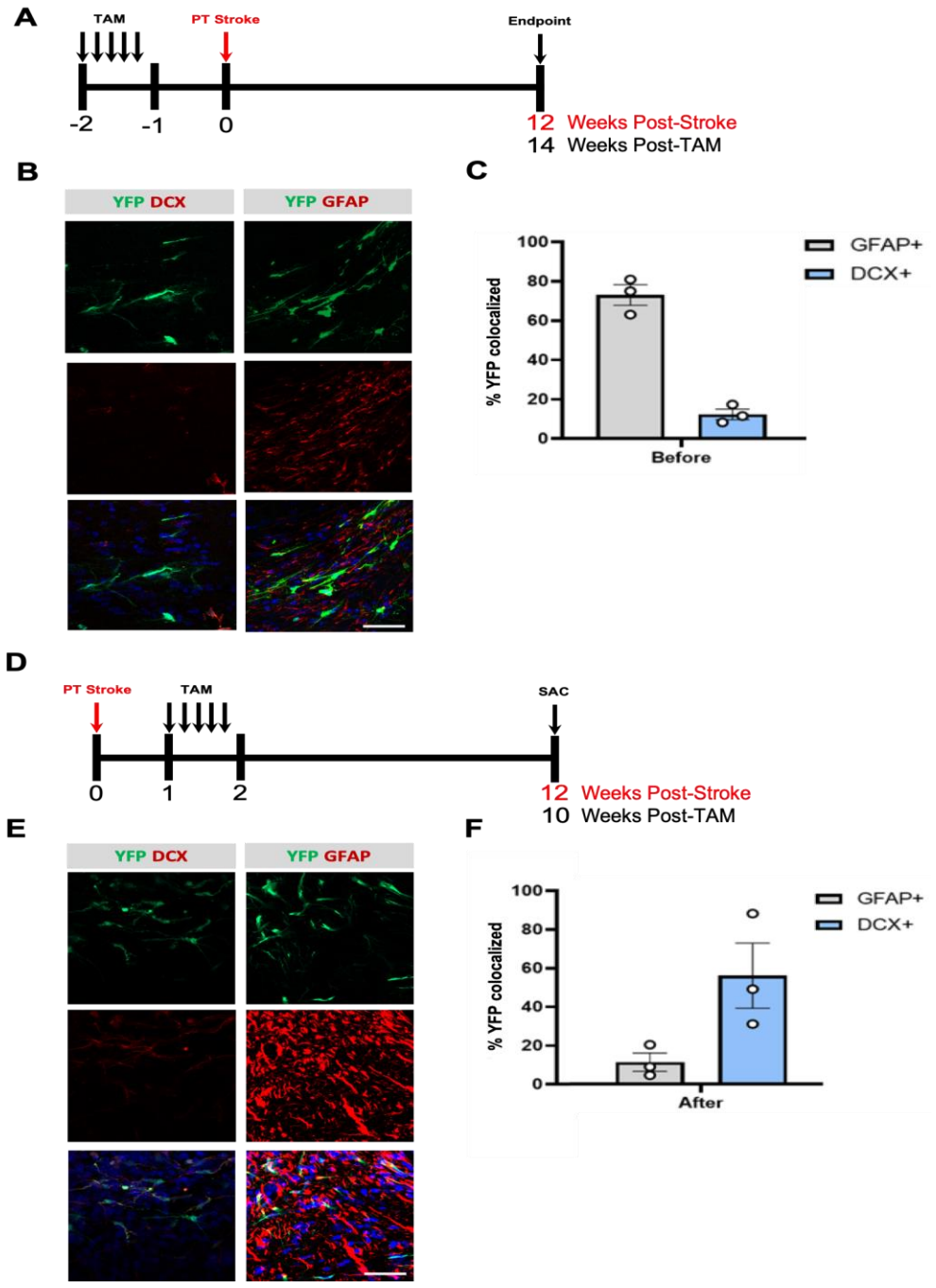


**Figure 1. SVZ-derived NSPCs labelled after stroke primarily take up a neuronal fate at 12 weeks post-stroke.** (A) Experimental timeline labelling nestin+ YPP-expressing cells before stroke in the nestinCreERT2-iBax mouse model (WT shown only). (B) Representative images of DCX and GFAP-expressing YFP+ cells labelled before stroke (n=3). (C) Quantification of YFP, DCX and GFAP shows a majority of nestin+ cells labelled before stroke express GFAP at the stroke site (n=3). (D) Experimental timeline labelling nestin+ cells after stroke (WT shown only). (E) Representative images of DCX and GFAP-expressing YFP+ cells labelled after stroke (n=3). (F) Quantification of YFP, DCX and GFAP shows a majority of nestin+ cells labelled after stroke express DCX at the stroke site (n=3). This data was modified from Ceizar et al. (2017).

**1.3d Regulation of NSPC Fate after Stroke**

There are several key factors involved in stroke-induced regulation of NSPC fate including the localization of NSPCs, changes to the microenvironment, as well as stroke-induced changes in NSPC transcriptional profiles. These factors will be reviewed here in order to begin to elucidate factors that may have contributed to our discovery that showed NSPCs labeled before stroke have an astrocyte fate, whereas those labeled after stroke have a neuronal fate.

As stated previously, the fate of naïve NSPCs can differ based off their post-migratory localization, with SVZ-derived NSPCs fated for the olfactory bulb differentiating into interneurons, whereas NSPCs migrating to the CC differentiating into oligodendrocytes (Bond et al., 2015). Given migration of the SVZ-derived NSPCs to the site of stroke injury is not the typical localization of these cells under naïve conditions it is possible that ectopic localization of NSPCs alters their fate. Work by Seindenfaden et al. (2006) tested this hypothesis and examined the fate of naïve NSPCs in ectopic regions in the brain through experiments that transplanted SVZ-derived NSPCs of naïve mice into different regions of the brain of other naïve mice. More specifically NSPCs were isolated from the SVZ of P75 mice and grafted into the striatum, motor cortex and lateral posterior thalamic nucleus of 6 to 10-week-old mice. Interestingly all the transplanted cells in all target regions had a glial fate. This was unexpected given the predominantly neuronal fate of SVZ-derived NSPCs migrating to the olfactory bulb and suggests the regions in which the cells localize has a role in determining NSPC fate. This study also showed that inducing the expression of neuronal markers in grafted cells was insufficient to induce a neuronal fate in the striatum which suggests that neuronal precursors have the ability to

differentiate into different cell types when localized in different environments. Together these findings highlight the stringent effect that the localization of NSPCs can have on fate specification.

Work by Benner et al. (2013) further characterized the stroke-induced changes to the microenvironment that promote astrogenesis. To this end, they employed the photothrombosis stroke model to show that following injury, there is enrichment of Thrombospondin-4 (Thbs4) in SVZ-derived NSPCs and upon migration to the site of injury where they primarily differentiate into astrocytes. They identify Thbs4 as an initiator of stroke-induced Notch signaling in the SVZ that also regulates the astrocytic fate of NSPCs migrating to the site of injury. Furthermore, they show blocking of this mechanism by knockout of Thbs4 was sufficient to induce a neuronal fate in migrating NSPCs.

The role of the microenvironment on NSPC fate post-stroke was also highlighted in recent work published by Pous et al. (2020). Using multiple stroke models, they showed that following stroke-induced disruption of the blood brain barrier and increases in vascular permeability, there is deposition of the coagulation factor, fibrinogen, in the SVZ and the site of injury. Fibrinogen has previously been shown to play a role in the inflammatory response in injury models (Petersen et al., 2018), but otherwise has not been implicated in NSPC fate choices following injury. Pous et al. (2020) identify that the deposition of fibrinogen following injury is sufficient to induce an astrocytic fate in Thbs4+ NSPCs derived from the SVZ and migrating to the site of injury, with reduced astrogenesis being observed following its depletion. Interestingly, the deposition of fibrinogen is specific to only up to 3 days post-stroke. Given the long-term migration of NSPCs to the site of injury, alongside the temporal presence of the fate-altering fibrinogen, this raises the possibility that temporal changes to the NSPC microenvironment are contributing to temporal

differences in fate observed following stroke. This remains to be tested since work by Pous et al. (2020) is restricted to examining the fate of NSPCs at only very early timepoints post-stroke when fibrinogen is present. Together, these studies come together to highlight the role of the NSPC microenvironment in determining NSPC fate following injury.

Although previous studies have characterized many different factors as playing a role in dictating NSPC-fate following stroke, none of these mechanisms easily explain why NSPCs labelled before stroke have an astrocyte fate versus those labeled after stroke have a neuronal fate. Therefore, this thesis addresses this question by elucidating the temporal roles of intrinsic regulators in determining NSPC-fate following stroke.

## 2. Objective and Hypothesis

**2.1 Objective:** Determine the intrinsic regulation dictating differences in neural stem and progenitor cell fate at the site of injury following stroke.

**2.2 Hypothesis:** Stroke induces temporal intrinsic changes that are sufficient to induce changes in fate uptake of SVZ-derived NSPCs at the site of injury.

# 3. Methods

### 3.1 General Animal Procedures

All animal procedures conducted were approved by the University of Ottawa Animal Care Committee and performed in accordance to the guidelines set out by the Canadian Council of Animal Care. Animals were housed in the University of Ottawa Animal Care and Veterinary Services facility. The housing rooms were maintained on a 12-hour light cycle at a temperature and humidity level of 23°C and 30%, respectively. Water and food were provided to the mice *ad libitum*.

### 3.2 nestinCreER$^{T2}$ Mouse Model

The nestinCreER$^{T2}$ mice were maintained at the University of Ottawa with the offspring consisting of mice that were heterozygous for nestinCreER$^{T2}$and R26R-eYFP allele (Dranovsky et al., 2011; Sahay et al., 2011).

### 3.3 Genotyping

All mice were genotyped at approximately 3 weeks of age to confirm zygosity of each transgene. Ear snips are collected and processed to isolate DNA by use of HotSHOT DNA extraction (Sigma). Ear snips were incubated for 30 minutes at 95$^{o}$C in Alkaine Lysis Buffer (25mM NaOH and 0.1mM $Na_2EDTA$), with Neutralization solution (40mM Tris-HCl) being added following incubation. Polymerase chain reaction (PCR) was performed using primers (Integrated DNA Technologies) to detect all transgenes. Following PCR, amplicons were electrophoresed on a 2% agarose gel stained with ethidium bromide and then imaged by use of ultraviolet illumination. PCR amplicon size was determined by referring to the standard DNA ladder (100bp ladder; DM001-R500M, Frogga Inc.).

### 3.4 Photothrombosis Surgery

A focal stroke was produced in the left motor cortex of mice by use of the photothrombosis stroke model, as per our previous publication (Kannangara et al., 2018). Briefly, mice were placed under a heat lamp, anesthetized by inhalation of 5% isoflurane and 1% oxygen, and given a subcutaneous injection of saline. The mice were mounted onto a stereotaxic frame with their body temperature being maintained throughout the surgery between 36.5 and 37.5°C using a rectal probe and feedback heating blanket (Harvard Apparatus). The scalp of mice was opened to expose the skull and the site of the stroke was mapped using coordinates +0.7 AP, +2.0 ML relative to the Bregma. Mice received an intraperitoneal injection of Rose Bengal (10mg/ml, R3877-5G; Sigma) and then 5 minutes after the injection, a green laser (532 nm, 25 mW, MGM20; Beta Instruments) located 3cm from the skull was used to irradiate the brain for 10 minutes. Following irradiation, the scalp was closed with Vetbond (3M), and 2% bupivacaine was administered as an analgesic immediately post-operation and 4 hours post-operation.

### 3.5 Tamoxifen Treatment

Mice were treated with tamoxifen (TAM) dissolved in 90% sunflower seed oil and 10% EtOH by use of intraperitoneal injections at a dose of 160mg/kg/day. Mice were treated for 5 consecutive days following stroke for all experiments except for the temporal lineage-tracing experiment where the mice receive one day of TAM treatment at varying times relative to stroke induction.

### 3.6 Transcardial Perfusion and Brain Collection

Mice were anesthetized using 0.05 mL of sodium pentobarbital (Euthanyl, 65 mg/mL). The mice were then transcardially perfused for 6 minutes with 1X phosphate-buffered saline (PBS) (4°C, pH 7.4, 7 mL/min), followed by 10 minutes with 4% paraformaldehyde (PFA) in 1X PBS (4°C, pH

7.4, 7 mL/min). Brains are removed and post-fixed in 4% PFA for one hour followed by being transferred into 30% sucrose with 0.1% sodium azide ($NaN_3$, 71290; Sigma) for cryoprotection.

**3.7 Fluorescent Immunohistochemistry**

Brains were sectioned at a thickness of 35 μm using a freezing microtome (SM 2010R; Leica) and collected in nine serial tubes filled with 1XPBS with 0.1% $NaN_3$ at 4°C. Free-floating immunohistochemistry was completed using matched sections collected from the caudal forelimb area (AP +1.0 to 0). The sections were rinsed in 1XPBS (3 x 5min), followed by blocking solution (3% normal donkey serum (NDS, 017-000-121; Jackson ImmunoResearch), 0.1% TritionX100 in 1XPBS). After blocking, sections were incubated in primary antibody in blocking solution for 24 hours shaking at 4°C using the following primary antibodies: GFP (Aves, 1:5000), Nestin (Cedarlane, 1:1000), Id2 (CalBioreagants, 1:1000), Ki67 (ESBE, 1:500), DCX (Santa Cruz, 1:5000), GFAP (Millipore, 1:500). The following day, sections were rinsed 1XPBS (3 x 5min), and incubated in the dark with Cy2, Cy3 and Cy5 conjugated secondary antibodies (Jackson ImmunoResearch, 1:500) in blocking solution and then rinsed in 1XPBS (3 x 5min). Sections were stained with the nuclear counterstain, 4',6-diamidino-2-phenylindole (DAPI, 10236276001; Sigma, 1:5000) for 5 minutes, rinsed in 1XPBS for 2 min and cover slipped with #1.5 coverslips using ImmuMount mounting medium (2860060; Fisher).

**3.8 Acquisition of images and quantification of cells**

All sections were blinded for experimental conditions and imaged using an epifluorescent confocal microscope at 40x magnification (University of Ottawa, CBIA Core Facility, Zeiss, LSM800 AxioObserverZ1). Manual cell counting was performed with optical z-plane sectioning in ZEN, with cells being quantified through examination of the entire Z-axis of sections that were imaged.

### 3.9 SVZ Isolation and Flow Cytometry

At endpoint, mice were injected with 0.05 mL of sodium pentobarbital (Euthanyl, 65 mg/mL) and the brains were quickly removed. SVZ was microdissected using a stereoscope according to our published protocol (Kannangara et al., 2018) and isolated in tubes containing artificial cerebrospinal fluid (ACSF) ($NaHCO_3$, 26mM; NaCl, 124mM; KCl, 5mM; $CaCl_2*2H_2O$, 2mM; MgCl2*6H2O, 1.3mM; MqWater). Following SVZ isolation, the ACSF was aspirated and replaced with digestion media (DMEM/F12; EDTA, 1.2mM; Papain, 20U/mL). The tissue was incubated for 30 minutes at 37$^oC$, followed by addition of resuspension media (DMEM/F12; DNASE 1, 0.5 mg/mL; FBS, 10%) and trituration five times using a P1000 pipette. Following trituration, Percoll-PBS solution (10:1 100% Percoll in 10X PBS) was added to tubes for a final concentration of 22% vol/vol Percoll and centrifuged for 13 minutes (500xg, 4$^oC$). After centrifugation, the supernatant was aspirated, and the cells were resuspended in DMEM/F12. YFP+ cells were then isolated from the single cell suspension using fluorescence-activated cell sorting (BeckmanCoulter MoFlo XDP). Dead cells were excluded by 7-AAD staining and 7AAD-negative live YFP+ cells were collected in DMEM/F12.

### 3.10 scRNAseq Library Preparation and Sequencing

Isolated YFP+ cells were processed with the 10x Genomics Single Cell 3' RNA-seq kit v3 at the OHRI StemCore Laboratories. Both gene expression libraries were prepared using the manufacturer's protocol, with gene expression libraries being sequenced to a depth of approximately 40-50,000 reads per cell.

### 3.11 scRNAseq Quality Control and Processing

Quality control and processing of both samples was performed using Seurat v3.1 package in R (Stuart et al., 2019). Respective expression matrices of the naïve and stroke samples were

processed using CellRanger, with cells containing a high percentage of mitochondrial gene expression being excluded from analysis. Expression values were normalized and scaled with the cell cycle scores, number of RNA molecules and percentage of mitochondrial reads all being regressed out. Principal component analysis was run on variable genes and the UMAP embeddings were calculated using the first 20 principal components and at a resolution of 0.2. Differential gene expression testing was performed using a non-parametric Wilcoxon rank sum test, with significant differential expression identified for genes with adjusted p-values < 0.05.

**3.12 GO Enrichment Analysis**

GO enrichment analysis was performed using the Gene Ontology Resource (Ashburner et al., 2000; The Gene Ontology Consortium, 2019). Briefly, all differentially expressed genes upregulated and downregulated in the Stroke sample were inputted to identify biological processes enriched in the Stroke sample. The most significant GO terms enriched were selected by identifying the GO terms with the highest adjusted p-value.

**3.13 iRegulon**

The regulon and master regulators of the regulon were established by use of iRegulon (Janky et al., 2014). Briefly, all differentially expressed genes upregulated and downregulated in the Stroke sample were inputted as nodes to identify enriched motif IDs and master regulators of enriched motif IDs.

**3.14 RNA Velocity Analysis**

RNA Velocity analysis was performed by use of the published scVelo workflow (La Manno et al., 2018; Bergen et al., 2020). Briefly, the data was preprocessed by normalizing cells by size, genes selected by minimum number of shared counts and variability, smoothing and using all sequenced cells to estimate the steady state ratio of spliced and unspliced molecules. Velocities

were determined and projected by modeling transcriptional dynamics of splicing kinetics onto the previously computed UMAP embeddings after calculating the dynamical model of both samples.

**3.15 Statistical Analyses**

All the data was plotted using the mean ± standard error of the mean (SEM). For analysis of 2 groups the two-tailed unpaired t-test was used. Analysis of more than 2 groups was completed using a two-way ANOVA with Bonferroni post-hoc. Statistical significance was set at $p < 0.05$.

# 4. Results

### 4.1 Temporally-specific fate mapping identifies post-stroke specificity of labelling neuronal-fated NSPCs

As described in the introduction, previous work in our laboratory had labeled NSPCs with TAM treatment for 5 days after stroke and showed these cells had a neuronal fate at the infarct (Ceizar, 2017). Given recent work supported that 1-3 days after injury NSPCs have an astrocytic fate due to changes in the microenvironment (Pous et al., 2020), a fate mapping assay was performed to determine the temporal specificity of labelling neuronal-fated NSPCs following stroke. To this end, the nestinCreER$^{T2}$ mouse model (Fig 2), was used to label NSPCs with one injection of TAM at varying timepoints before vs. after stroke (7 days pre-stroke, 2 days post-stroke, 7 days post-stroke, 14 days post-stroke) (Fig 3). One injection of TAM was administered in order to allow for temporal precision of labeling NSPCs, which was difficult to attain using our previous paradigm involving 5 days of TAM treatment. The fate of the labelled NSPCs surrounding the infarct was determined 14 days following TAM treatment. Imaging and quantification of YFP+ cells colocalizing with DCX and GFAP was used to assess the phenotype of cells in relation to when the labelling occurred relative to stroke induction (Fig 4). When labelling occurred at 7 days pre-stroke, as well as 2 and 7 days post-stroke the majority of the migrated YFP+ cells had an astrocytic phenotype and expressed GFAP. In contrast when labeling 14 days post-stroke almost 50% of the cells had a neuronal phenotype and expressed DCX. This result highlights that the fate specification of NSPCs is in fact temporally specific and is in agreement with previous work (Pous et al., 2020) showing NSPCs differentiate into astrocytes within the first 7 days after injury.

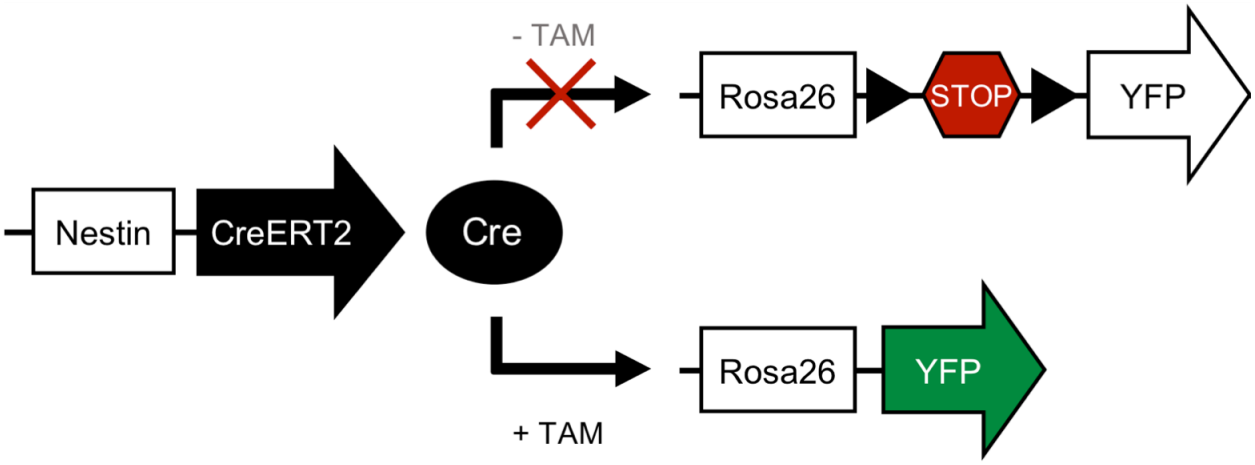


**Figure 2. Tamoxifen-Induced recombination in the nestinCreER$^{T2}$ mice.** (A) A double transgenic nestinCreER$^{T2}$ mouseline was produced by breeding the inducible nestinCreER$^{T2}$ mouse with the R26R-YFP reporter mouse.

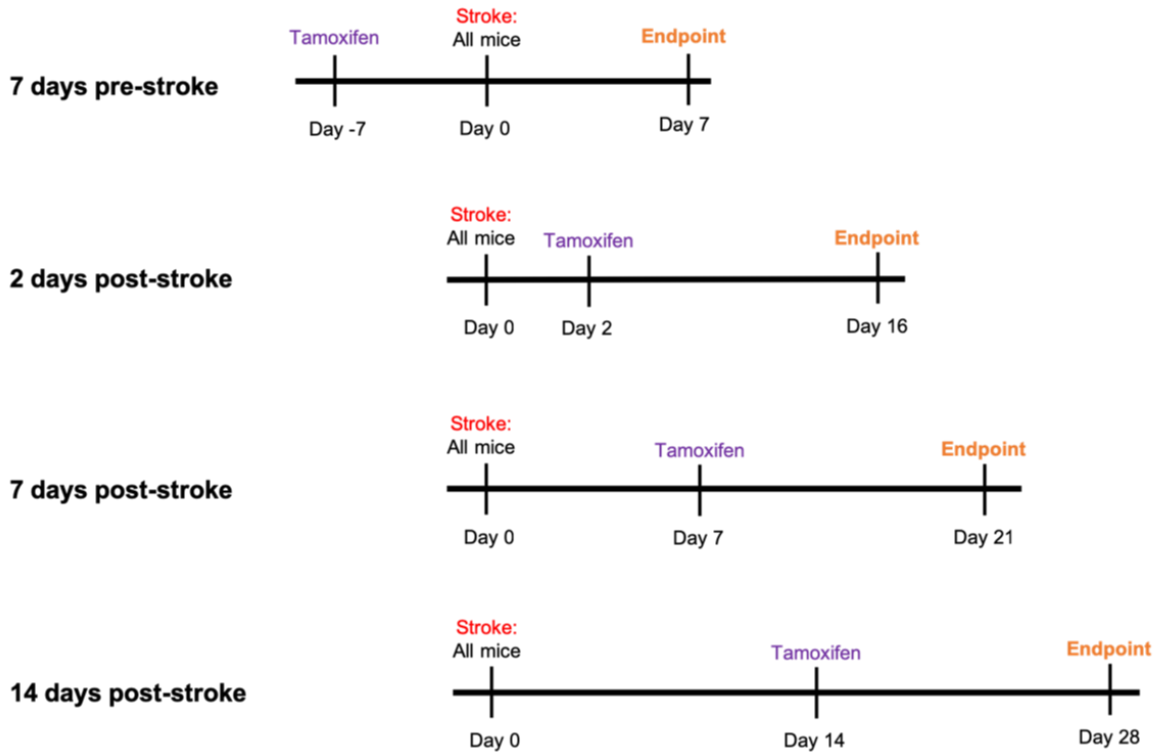


**Figure 3. Temporal-specific lineage tracing timeline.**

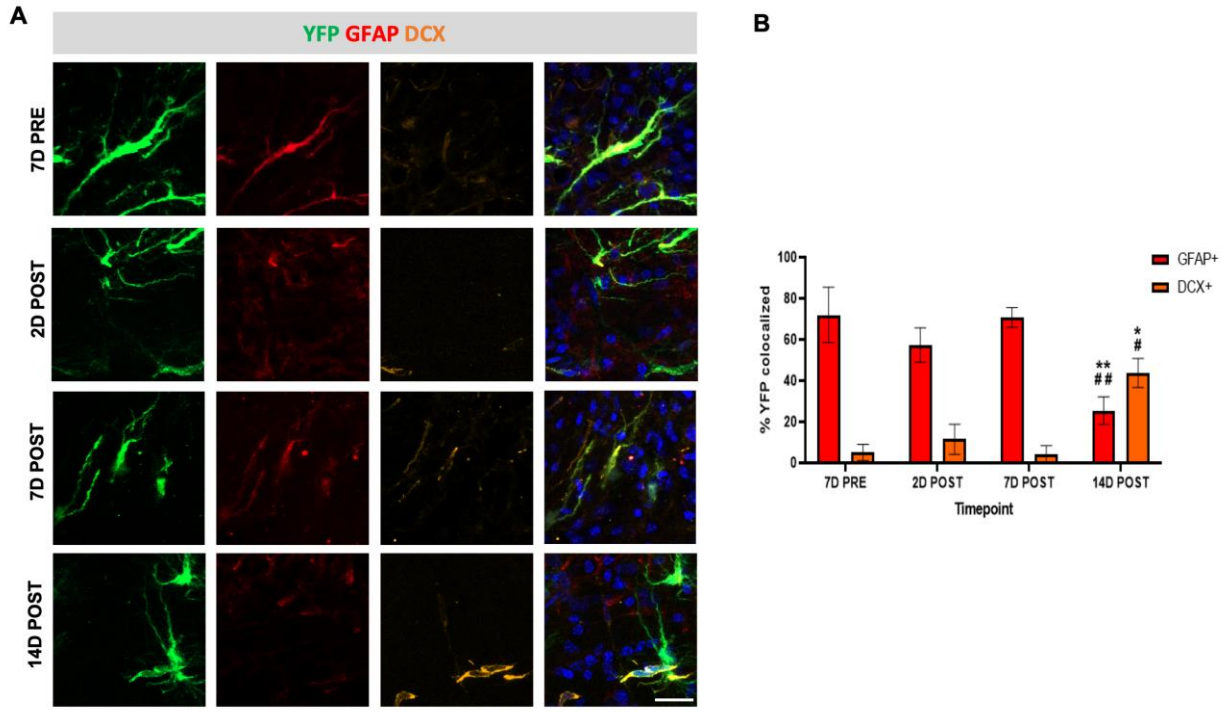


**Figure 4. Stroke induces temporal-specific increase in proportion of DCX+ YFP+ migrating cells at the site of stroke.** (A) Representative images showing immunohistochemical characterization of recombined YFP+ cells expressing GFAP and DCX following stroke. Scale bar, 20um. (B) Quantification of recombined YFP+ cells expressing GFAP and DCX following stroke shows temporal switch in fate specification relative to stroke induction (n=3). *p<0.05, **p<0.01 represents significance from 7D PRE. # = significance from 7D POST.

**4.2 Single cell RNA sequencing of SVZ-derived neural stem and progenitor cells**

scRNAseq was performed to identify what cell populations arise from nestin+ NSPCs labelled after stroke and if there are differential transcriptional profiles present in the labelled cells at the SVZ. Specifically, cells labelled after stroke (hereafter referred to as stroke group) were compared to cells labelled under naïve conditions, as occurred when cells were labeled before stroke (hereafter referred to as naive group) (Fig 5). Fluorescence-activated cell sorting (FACS) was performed 5 days following tamoxifen treatment to isolate living (7-AAD negative) YFP+ cells from the SVZ of naïve and stroke mice (Fig 6). In total, approximately 33,000 cells from the SVZ of 2 naïve mice, and approximately 26,000 cells from the ipsilateral SVZ of 2 stroke mice were isolated. These cells were subjected to droplet-based scRNAseq using the 10x Genomics Chromium platform. The number of reads per cell was approximately 45,000 per cell, with a sequenced output of 7,207 and 6,123 cells being generated from naive and stroke samples, respectively.

Unsupervised clustering for both samples was performed with dimensional reduction by uniform manifold approximation and projection (UMAP) (Fig 7). Clusters were classified by enrichment for cluster-specific genes as per previously published work (Llorens-Bobadilla et al., 2015; Dulken et al., 2017; Basak et al., 2018; Kalamakis et al., 2019) (Fig 8). Identified clusters included neural stem cells (NSCs) (*Aldoc, Slc1a3, Fabp7*+), transit amplifying progenitors (TAPs) (*Top2a, Hmgb2*+), early neuroblasts (eNBs) (*Ccnd2, Sox4*+), and late neuroblasts (lNBs) (*Dcx, Stmn2*+). There was also very low number of cells in 4 other clusters that were identified as medium spiny neurons (MSNs) (*Pcp4*+), oligodendrocytes (Oligos) (*Mal*+), ependymal cells (*Tmem212*+), and pericytes (*Vtn*+) (Fig 9). These latter cell types were not expected to be labelled

and were likely labelled due to nonspecific recombination, and thus removed from downstream analysis.

Based on previous studies having identified that NSPCs are a diverse group of cells (Llorens-Bobadilla et al., 2015; Dulken et al., 2017; Basak et al., 2018; Kalamakis et al., 2019), re-clustering was performed on clusters of the NSPC lineage (Fig 10). This analysis identified one group of quiescent neural stem cells (qNSCs) and three subpopulations of activated neural stem cells (aNSCs). Furthermore, there was two subpopulations of TAPs, and one group of NBs. The aNSC subpopulations consist of: a) aNSCs 1 which is defined by increased transcription and RNA synthesis genes such as Rpsa and Rpl32 relative to qNSCs; b) aNSCs 2 which is defined by increased expression of activation initiators such as Sox4 and Sox11 relative to aNSCs 1, and lastly; c) aNSCs 3 which is defined by increased expression of proliferative genes relative to aNSCs 2. The TAPs were defined by increased expression of cell cycle genes relative to the aNSC clusters, with the cells in G2M phase of the cell cycle labelled as TAPs 1, where those that are in S phase are labelled as TAPs 2.

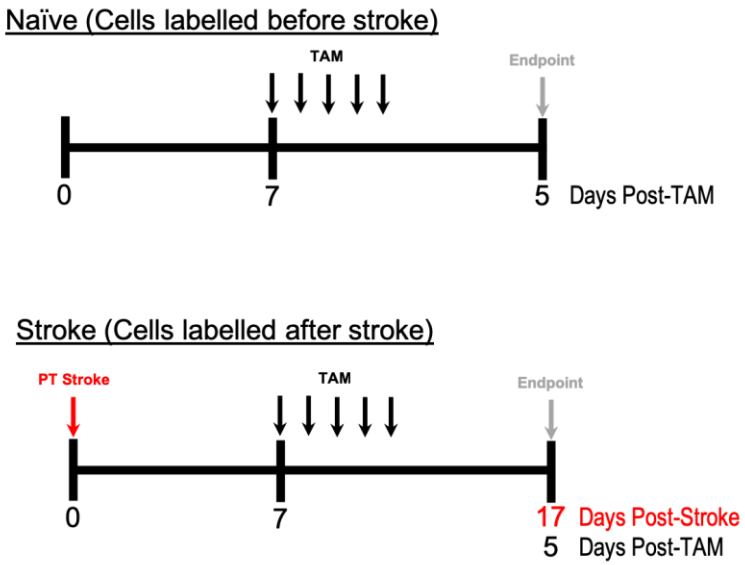


**Figure 5. scRNAseq experimental timeline.**

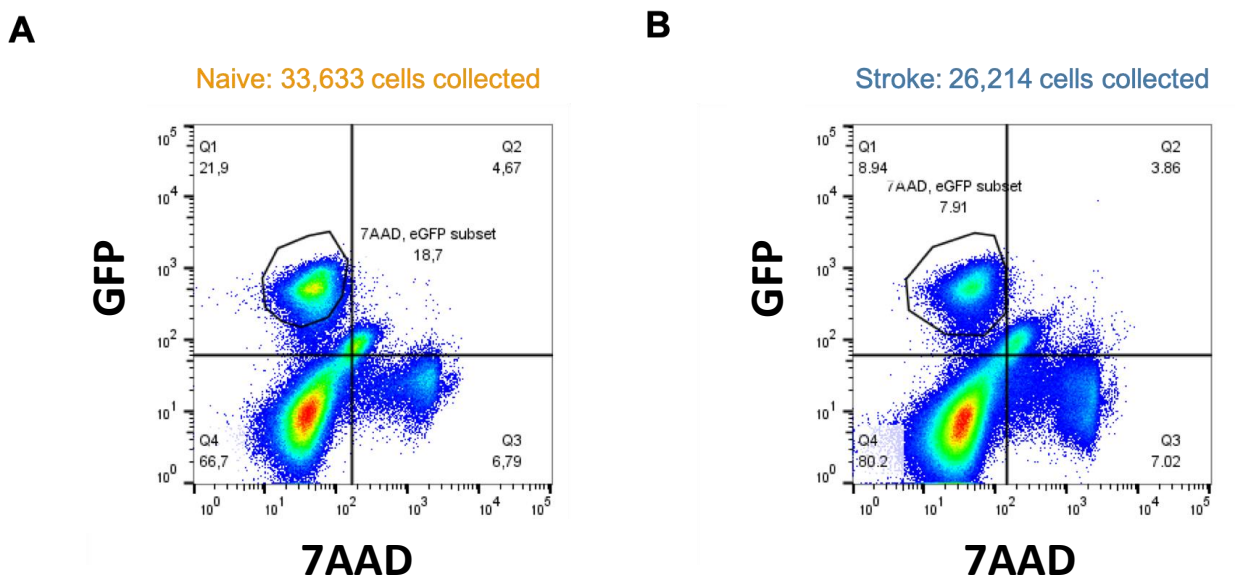


**Figure 6. FACS gating strategy for isolation of live YFP+ cells.** (A) FACS gating on cells sorted from naïve samples. (B) FACS gating on cells sorted from stroke samples. Quadrants gated are defined as: Q1, eGFP+ 7AAD-; Q2, eGFP+ 7AAD+; Q3, eGFP- 7AAD+; Q4, eGFP- 7AAD-.

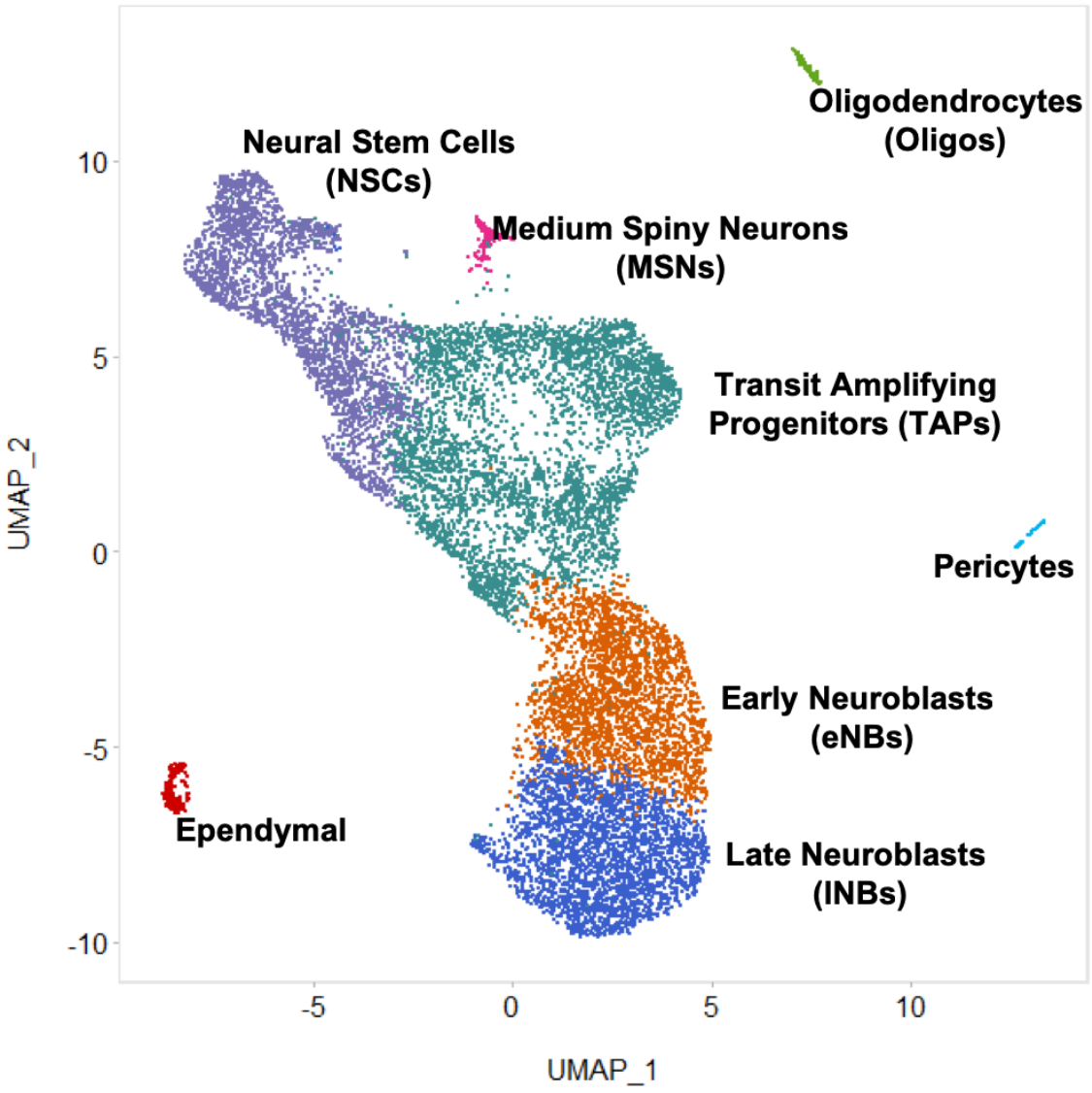


**Figure 7. UMAP dimensional reduction identifies eight cell clusters in scRNAseq samples.**

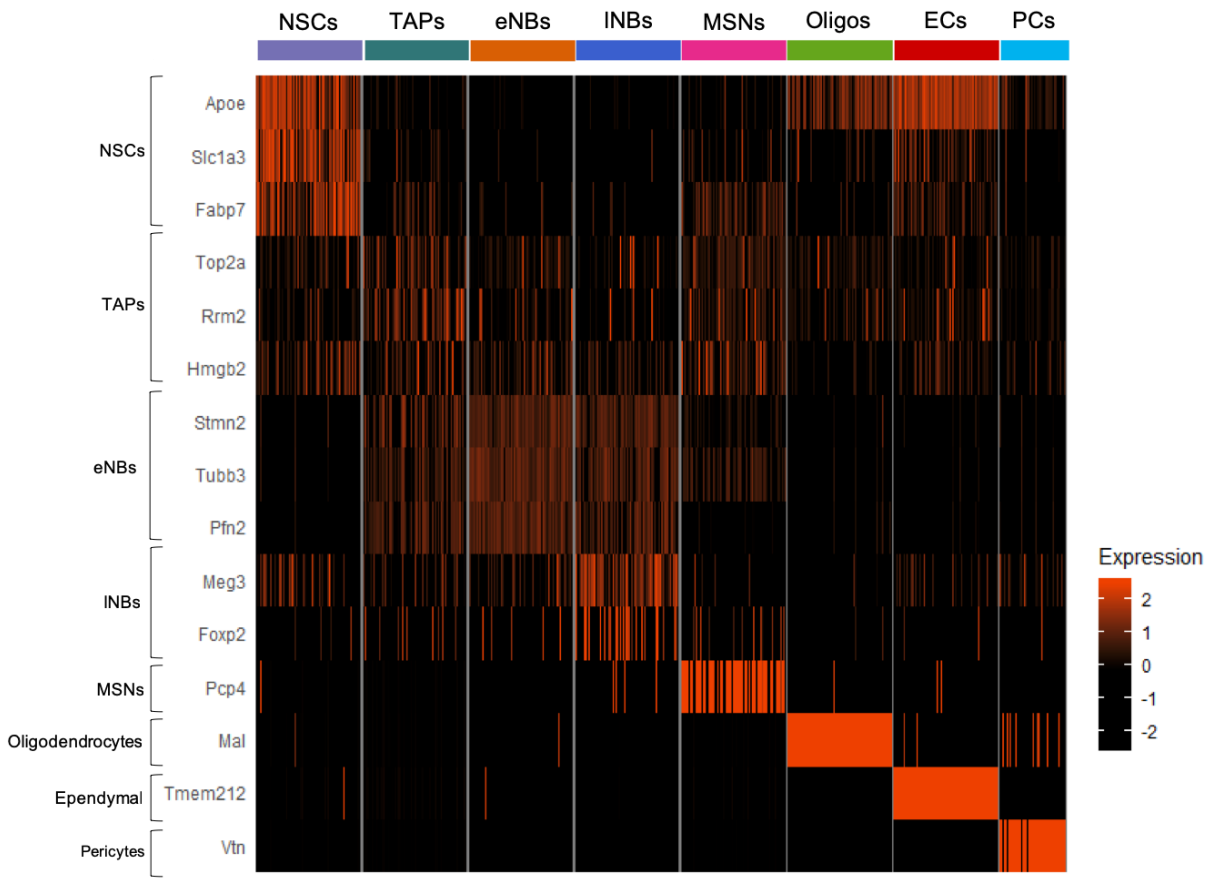


**Figure 8. Differential gene expression analysis visualized by heatmap shows cluster-specific enrichment of select genes as population markers.**

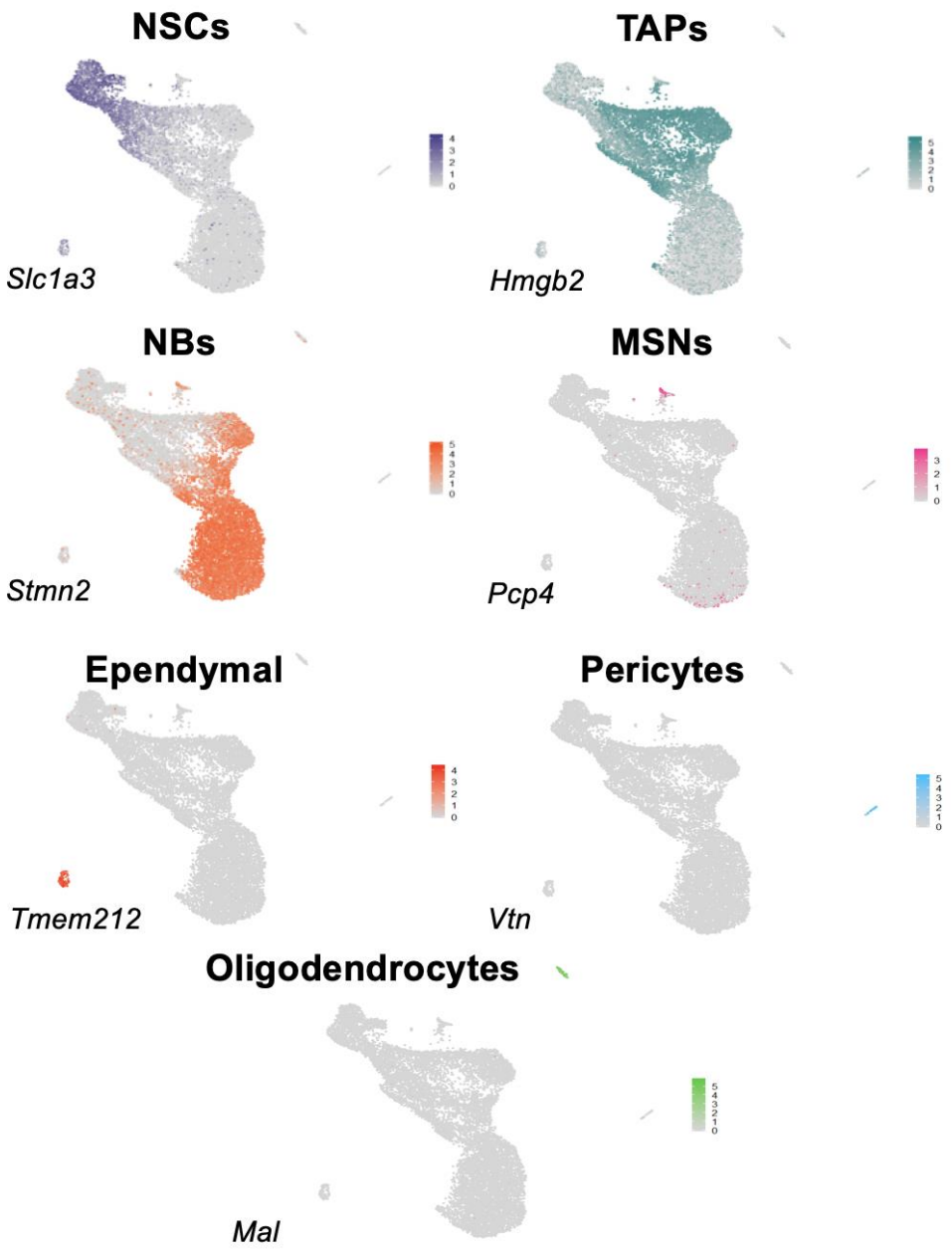


**Figure 9. UMAP dimensional reduction shows representative cell-specific expression of transcript within clusters of enriched genes as population markers.**

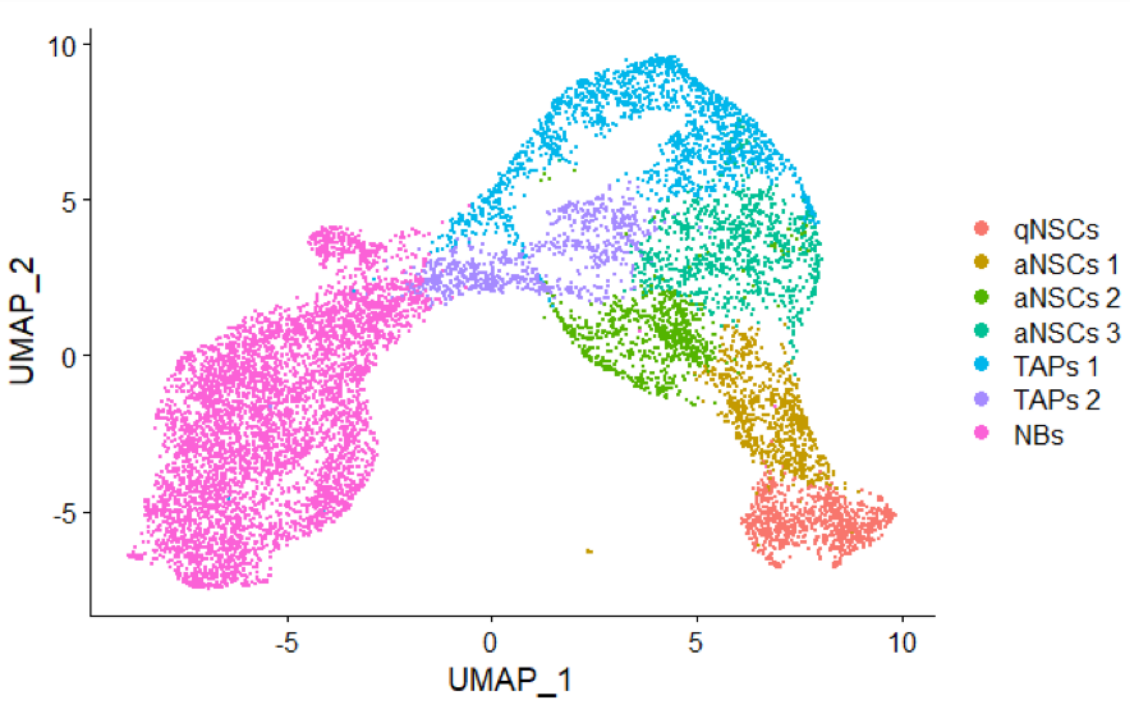


**Figure 10. Subset analysis of the NSPC lineage introduces re-clustering of cells sequenced.** UMAP dimensional reduction of the neuronal lineage identifies seven cell clusters.

### 4.3 Single cell transcriptomics reveals decreased proportion of NSPCs labelled after stroke found in a quiescent state

Dimensional reduction showed that both the naive and stroke samples contain cells within all 7 defined clusters, suggesting that the same cells at the SVZ are labeled 5 days after TAM treatment, independent of whether the mice had a stroke (Fig 11). The stroke sample compared to the naïve sample however had a lower proportion of qNSCs, which has been previously reported to occur in other injury models (Llorens-Bobadilla et al., 2015). This reduction in qNSCs was accompanied by an increased proportion of NBs, in the absence of any prominent differences in any of the aNSC and TAP clusters between samples. Together, this data highlights the stroke-induced changes occurring in the SVZ including decreases in the proportion of qNSCs present.

Immunohistochemical characterization was used to confirm the differences of proportional contribution of cell types observed between groups in the scRNAseq dataset. This was done on tissue obtained from mice processed according to the timelines defined in Figure 5. Staining for YFP+Nestin+ cells, which includes aNSCs and TAPs, and not qNSCs or NBs (Codega et al., 2014), was performed to identify if there are differences in the proportions of nestin+ NSPCs after stroke (Fig 12). Quantification of YFP+Nestin+ cells shows no difference in the proportion of YFP+Nestin+ cells labelled after stroke.

Given the scRNAseq data showed a reduced proportion of qNSCs present in the NSPCs labelled after stroke, immunohistochemical characterization was performed for YFP+Id2+ cells to test if there is a significant difference in proportion of qNSCs *in vivo* (Llorens-Bobadilla et al., 2015). In agreement with the scRNAseq data there was a significant decrease in the proportion of the YFP+ population expressing Id2 in the stroke sample (Fig 13). These data strongly suggest that there is a reduction in qNSCs after stroke as identified by these scRNAseq and histological

analysis, which are in agreement with previous scRNAseq reports showing a reduced proportion of qNSCs in the SVZ following ischemic injury (Llorens-Bobadilla et al., 2015).

Previous reports show increases in proliferation in the SVZ following stroke (Arvidsson et al., 2002; Palma-Tortosa et al., 2017), yet our scRNAseq dataset did not reveal any significant differences in the proportion of TAPs 1 and TAPs 2 labelled between the naïve and stroke samples. To test if there is a difference in proportion of proliferating NSPCs labelled following stroke, we performed immunohistochemical analysis to examine the number of YFP+ cells that expressed the cell cycle marker Ki67 (Sarli et al., 1994) in the SVZ (Fig 14). Quantification of KI67+ cells colocalized with YFP revealed no difference in the proportion of YFP+Ki67+ cells between naïve and stroke mice, which is in line with the output of the scRNAseq analysis.

The adult SVZ has different areas within it that are formed from multiple structures that arise during development including the pallium, the lateral ganglionic eminence and the medial lateral ganglionic eminence (Chaker et al., 2016). Therefore, we also tested if the embryonic origin of cells being labelled following stroke differs to those labelled in the naïve sample. In adulthood, the embryonic origin of different regions can be identified by use of markers of these origins. For example, cells derived from the pallium can be identified by Emx1 expression, cells from the lateral ganglionic eminence by Gsx2 expression, and cells from the medial ganglionic eminence by Nkx2-1 expression, as reviewed by (Chaker et al., 2016). Using the scRNAseq dataset, we observe that both the naïve and stroke samples express primarily Gsx2, which is indicative that they originated from the lateral ganglionic eminence (Fig 15). This finding supports that cells of the same embryonic origin are being labelled before versus after stroke.

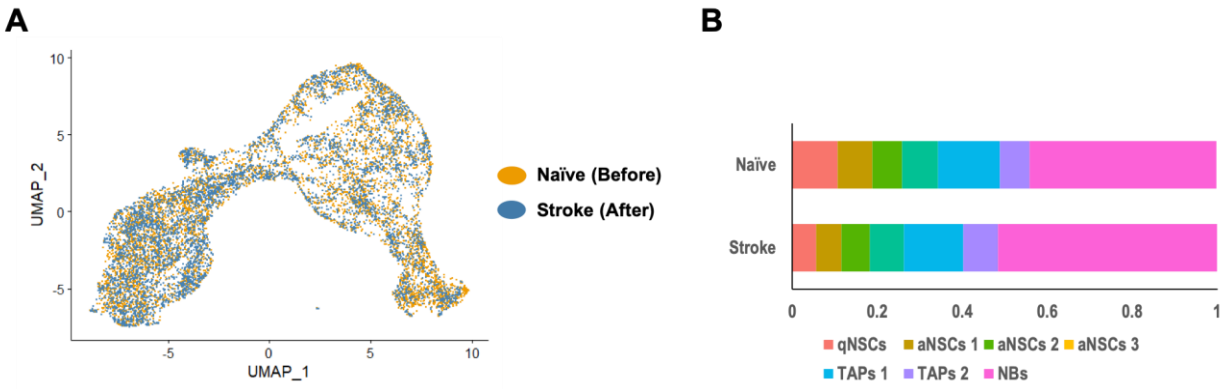


**Figure 11. Subset analysis of NSPCs identifies decreased qNSC and increased NB proportions following stroke.** (A) UMAP dimensional reduction shows cells from both naive and stroke mice in all seven cell clusters. (B) Analysis of sample composition identifies greater proportion of NBs, and lower proportion of qNSCs in stroke mice.

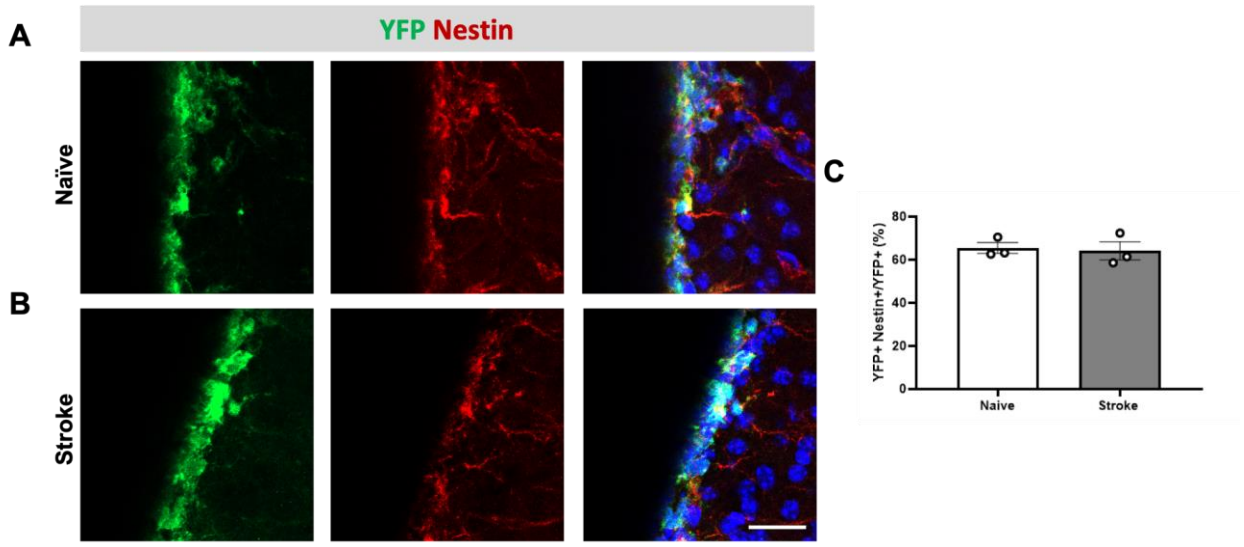


**Figure 12. Number of YFP+ nestin-expressing NSPCs labelled after stroke does not differ post-stroke.** Representative images showing recombined YFP+ nestin-expressing NSPCs in the SVZ of (A) naïve mice and (B) stroke mice. Scale bar, 20um. (C) Quantification of recombined YFP+ nestin-expressing NSPCs in the SVZ show no differences in the number of YFP+ nestin-expressing NSPCs post-stroke.

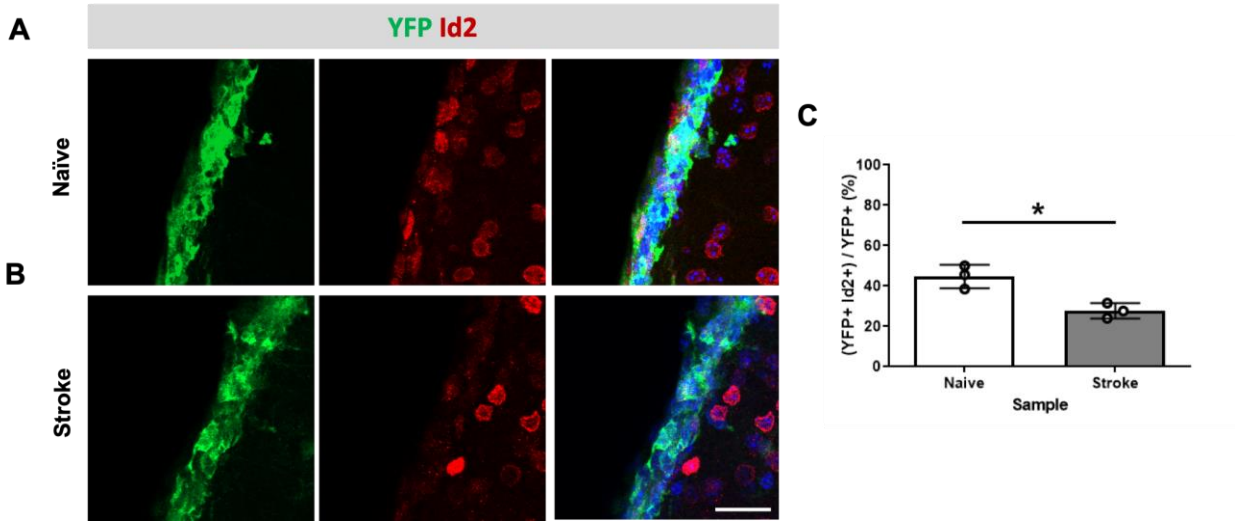


**Figure 13. Proportion of YFP+ Id2+ cells labelled is reduced following stroke.** Representative images showing recombined YFP+ Id2+ cells in the SVZ of (A) naïve mice and (B) stroke mice. Scale bar, 20um. (C) Quantification of recombined YFP+ Id2+ cells in the SVZ show a reduced proportion of YFP+ Id2+ cells in the SVZ post-stroke. *p<0.05.

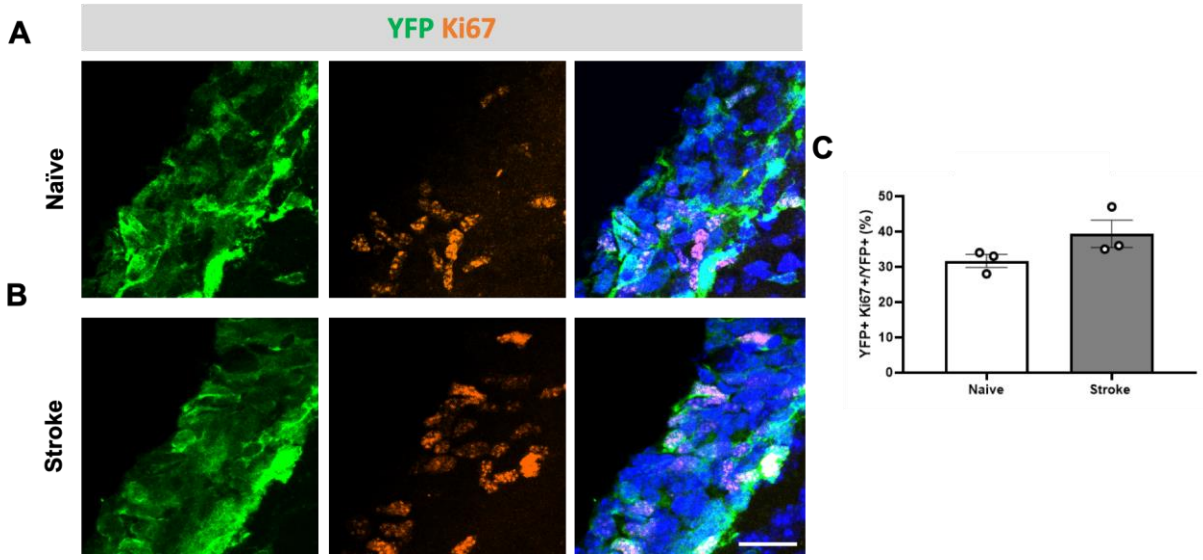


**Figure 14. Proportion of YFP+ Ki67+ cells labelled does not differ following stroke.** Representative images showing recombined YFP+ Ki67+ cells in the SVZ of (A) naïve mice and (B) stroke mice. Scale bar, 20um. (C) Quantification of recombined YFP+ Ki67+ cells in the SVZ shows no changes in proportion of YFP+ Ki67+ cells in the SVZ post-stroke.

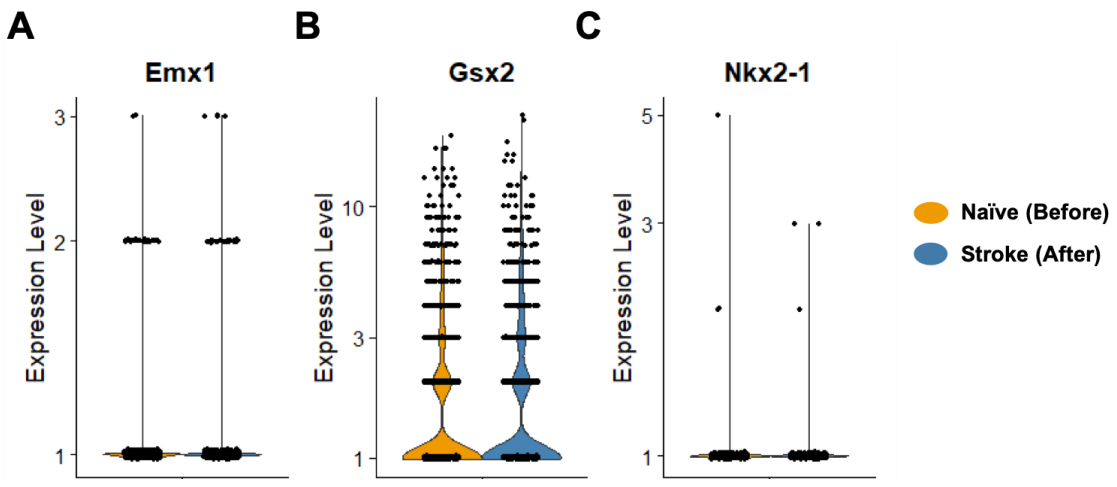


**Figure 15. No difference in embryonic origin of cells labelled after stroke.** (A) Expression level of Emx1 in qNSCs and aNSCs from naïve and stroke mice. (B) Expression level of Gsx2 in qNSCs and aNSCs from naïve and stroke mice. (C) Expression level of Nkx2-1 in qNSCs and aNSCs from naïve and stroke mice.

### 4.4 Increased proportion of NBs at the SVZ following stroke fated to become periglomerular neurons

In alignment with our previous histological assessments showing more NBs surround the infarct after stroke (Ceizar, 2017), there was a higher proportion of NBs in the stroke samples sequenced for scRNAseq analysis. Given the scRNAseq dataset suggested a large increase in the proportion of NBs in the SVZ following stroke, we performed staining for YFP+DCX+ at the SVZ in order to confirm and quantify this result (Fig 16). Quantification of YFP+DCX+ shows a trend ($p=0.056$), with there being a larger proportion of YFP+ cells colocalizing with DCX in the SVZ. This finding suggests that the increase in neuronal fated cells in the peri-infarct region when NSPCs are labeled after stroke, is preceded by an increased proportion of NSPCs that have developed into NBs in the SVZ before emigration.

As fate mapping of the adult SVZ has identified that NSPCs reside in multiple different transcription factor domains that generate specific neuronal subtypes (Chaker et al., 2016), we proceeded to identify if there are specific subtypes of neurons being produced following stroke. To this end, the expression of the transcription factors that identify NBs fated to become periglomerular neurons (Sp8, Pax6), deep granule neurons (Nkx2-1), glutamatergic juxtaglomerular interneurons (Neurog2), and type 1-4 interneurons (Nkx6-2) were analyzed within our scRNAseq dataset (Fig 17). Both the naïve and stroke sample were enriched for Sp8 and Pax6 expression, which are both associated with domains from which periglomerular neurons fated for the olfactory bulb are derived (Kohwi et al., 2005; López-Juárez et al., 2013). In contrast, transcription factors for the other cell types had low, or no expression in either the naïve or stroke sample. This finding suggests that cells from the naïve and stroke sample are derived from the periglomerular domain. This is supported also by previous published findings

from our lab that showed the migrated NSPCs after stroke in reporter Nestin-GFP mice have electrophysiological characteristics suggestive of periglomerular neurons (Kannangara et al., 2018).

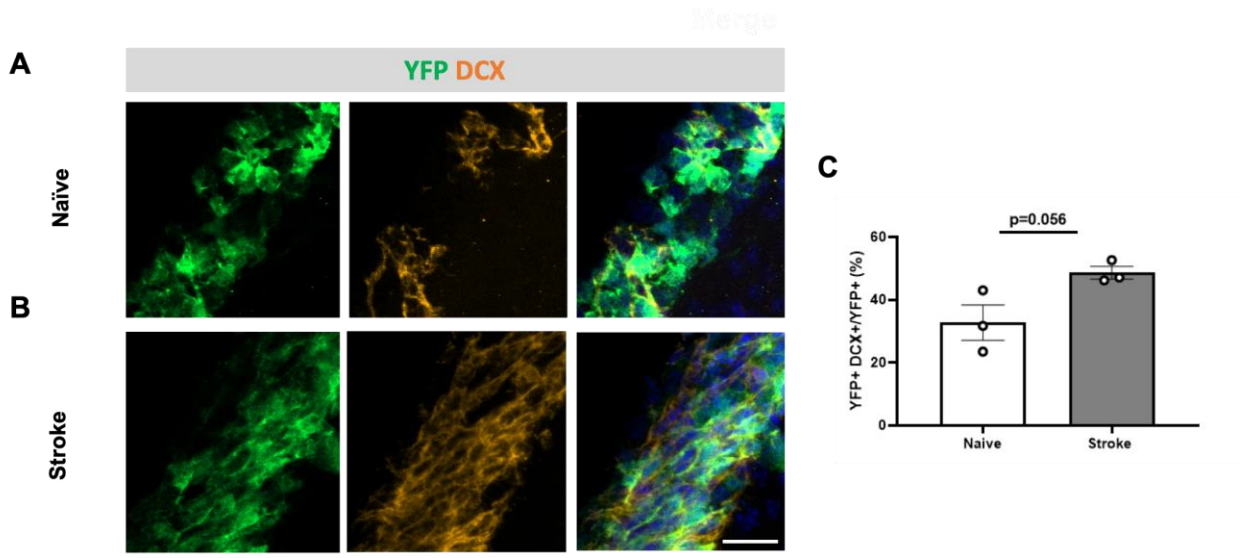


**Figure 16. Proportion of YFP+ DCX+ cells labelled is increased following stroke.** Representative images showing recombined YFP+ DCX+ cells in the SVZ of (A) naïve mice and (B) stroke mice. Scale bar, 20um. (C) Quantification of recombined YFP+ DCX+ cells in the SVZ shows increased proportion of YFP+ DCX+ cells in the SVZ post-stroke.

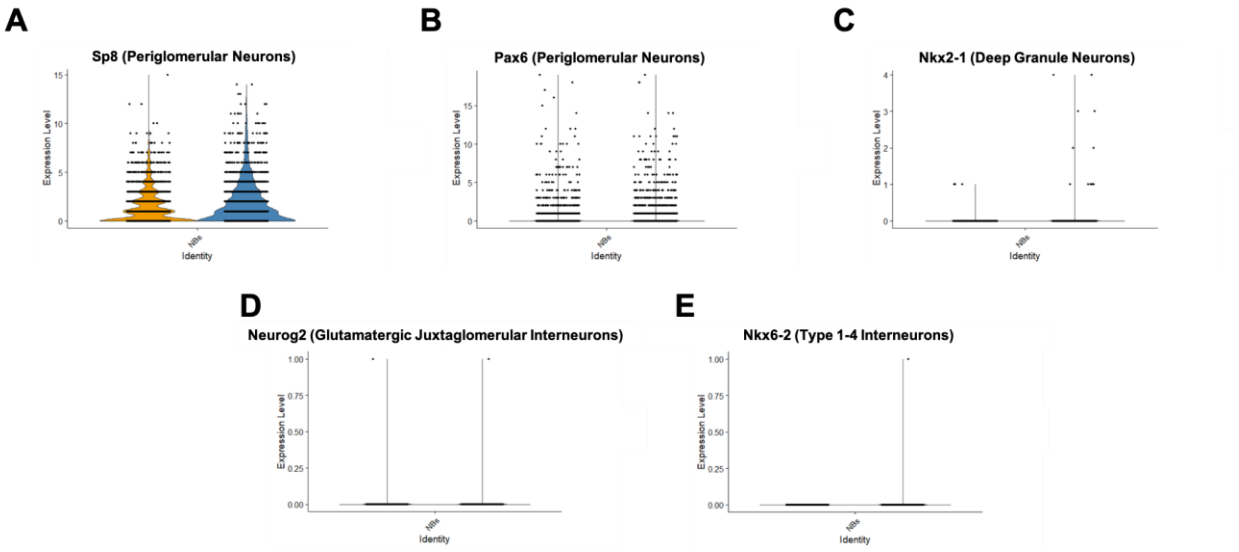


**Figure 17. No difference in NB subtypes produced following stroke.** (A) Expression level of Sp8 in sequenced YFP+ cells from naïve and stroke mice. (B) Expression level of Pax6 in sequenced YFP+ cells from naïve and stroke mice. (C) Expression level of Nkx2-1 in sequenced YFP+ cells from naïve and stroke mice. (D) Expression level of Neurog2 in sequenced YFP+ cells from naïve and stroke mice. (E) Expression level of Nkx6-2 in sequenced YFP+ cells from naïve and stroke mice.

### 4.5 Single cell transcriptomics reveals stroke-induced neuronal transcriptional profile in NSPCs

Another aim of performing scRNAseq on isolated YFP+ SVZ cells labelled after stroke was to perform an unbiased search for differences in the transcriptional profile of NSPCs in the naïve versus stroke sample. Following sequencing and cluster classification, Gene Ontology (GO) term enrichment analysis (Ashburner et al., 2000; Mi et al., 2019; The Gene Ontology Consortium, 2019) was performed on genes differentially expressed after stroke to identify perturbed biological functions by enrichment for their respective gene sets. As shown in Figure 18, analysis of genes up- and down-regulated in the stroke sample was compared to the naïve sample and shown as GO terms enriched relative to the stroke sample. Examination of the significantly enriched GO terms showed that neuron differentiation was one of the significantly overrepresented GO terms after stroke. The observed enrichment in neuron differentiation was due to upregulation of neuronal genes including Dlx1, Dpysl2 and Marcksl1. Furthermore, our GO Term analysis also identified that genes that regulate astrocyte differentiation as one of the most significant group of genes that are downregulated in the stroke sample. This group of genes included genes, such as Id1, Klf4 and Hes5. Together these findings show that the global profile of sequenced NSPCs after stroke is one that would favour a neuronal fate in these cells, which falls in line with labelling NSPCs after stroke primarily labeling cells fated to become neurons.

Given GO term analysis was performed using all cells sequenced in both samples, analysis was also performed to identify if the enriched GO terms are associated with a specific cell cluster or if they are associated with the entire samples sequenced. To elucidate the differential expression of these genes between cell populations we performed pseudotemporal ordering of transcriptional dynamics of the sequenced cells (Trapnell et al., 2014; Qiu et al., 2017a; Qiu et al.,

2017b) (Fig 19). Analysis of astrocytic gene expression shows that the downregulation of astrocyte genes occurs within the NSC end of the continuum, and not across all cell types. The pseudotime analysis also revealed that the enrichment of neuronal gene transcription is not specific to a single cell type but is observed across the entire NSPC lineage.

Further analysis of the scRNAseq dataset was performed using iRegulon, to identify potential master regulators of the differentially expressed genes after stroke (Janky et al., 2014). This analysis works by identifying enriched motifs in the gene set, with the transcription factors that target these motifs and thus potentially regulating the observed differential expression being identified. Shown in Figure 20 are the top 5 hits for potential master regulators of genes either upregulated or downregulated after stroke, respectively. Interestingly in both upregulated and downregulated gene sets following stroke, serum response factor (Srf), a transcription factor implicated in fate-specification, is suggested as a potential regulator (Lu and Ramanan, 2012). Further work examining the roles of such transcription factors following stroke in NSPC-fate decisions would allow for identifying a novel mechanism regulating NSPC fate.

Together, these findings suggest after stroke that there is a transcriptional profile where NSCs have upregulation of neuronal differentiation and downregulation of astrocyte differentiation, and then sustained upregulation of neuronal differentiation throughout the NSPC lineage. This highlights that NSPCs labelled following stroke as having a neuronal-fated profile present at the transcriptional level to a further extent than in NSPCs labelled under naive conditions.

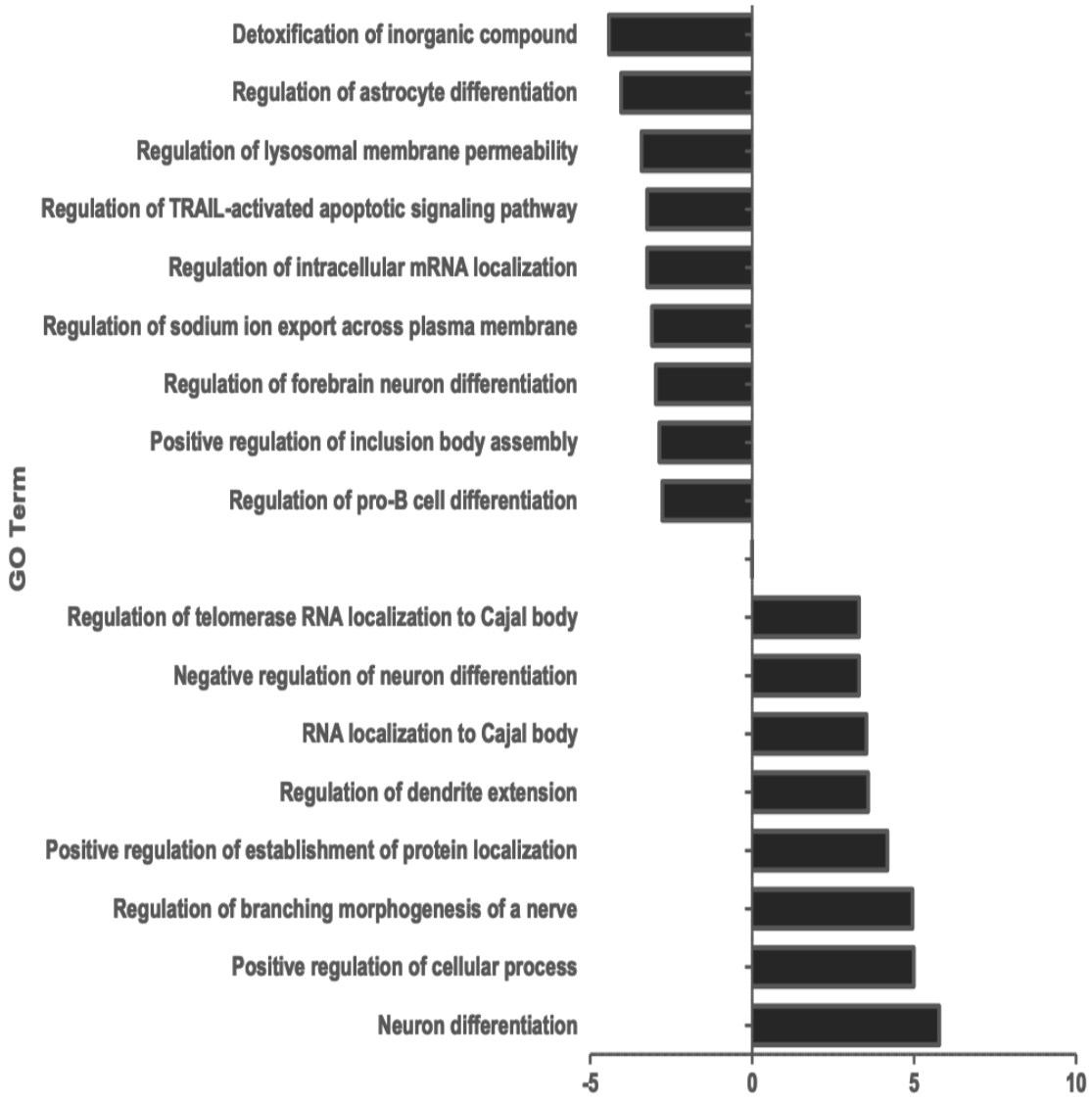


**Figure 18. Gene set enrichment for genes differentially expressed in cells labelled after stroke.** Enrichment plotted by adjusted p-value. GO terms with negative values represent GO terms overrepresented from the genes downregulated, with positive values representing GO terms overrepresented from the genes upregulated after stroke.

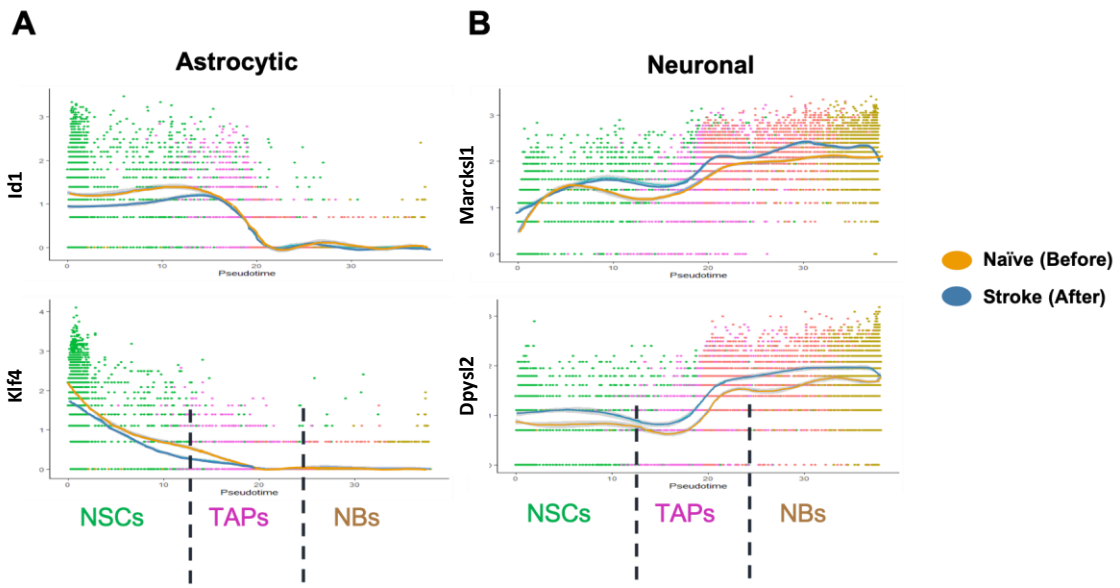


**Figure 19. Pseudotemporal analysis reveals decreased astrocytic gene expression in NSCs and increased neuronal gene expression in NSPCs labelled after stroke.** (A) Pseudotime trajectory analysis of astrocyte gene expression across clusters shows decreased expression in NSCs labelled after stroke. (B) Pseudotime trajectory analysis of neuronal gene expression across clusters shows increased expression in all cell types labelled after stroke.

**A**

Master Regulators of Downregulated Genes Post-Stroke

| TF | NES | #Targets | #Motifs/Tracks |
|---|---|---|---|
| Sox11 | 6.490 | 90 | 25 |
| Yy1 | 5.669 | 84 | 5 |
| Sox6 | 5.121 | 59 | 4 |
| Srf | 4.849 | 120 | 5 |
| Etv3 | 4.113 | 19 | 2 |

**B**

Master Regulators of Upregulated Genes Post-Stroke

| TF | NES | #Targets | #Motifs/Tracks |
|---|---|---|---|
| Mef2a | 4.644 | 82 | 3 |
| Srf | 4.474 | 78 | 15 |
| Polr2a | 4.228 | 104 | 6 |
| Atf3 | 4.175 | 126 | 21 |
| Hlf | 3.852 | 107 | 9 |

**Figure 20. Gene regulatory network analysis reveals master regulators underlying differential gene expression following stroke.** (A) Transcription factors associated with enriched motifs of genes downregulated following stroke. (B) Transcription factors associated with enriched motifs of genes upregulated following stroke. TF, transcription factor; NES, normalized enrichment score.

### 4.6 Single cell transcriptomics reveals no difference in global RNA velocity and rate of transition

Given the previous scRNAseq analysis provides a static snapshot of the cells sequenced, RNA velocity analysis was performed to better understand the time-resolved differences and cellular dynamics present following stroke. RNA velocity is a vector consisting of the time derivative of the gene expression state that is used to predict the future transcriptional state of cells, by determining the steady-state ratio of genes by isolating spliced and unspliced mRNAs sequenced in the scRNAseq dataset (La Manno et al., 2018). For the naïve and stroke sample the scVelo pipeline (La Manno et al., 2018; Bergen et al., 2020) was used to determine the RNA projection velocity which was superimposed on UMAP embeddings to predict the cell lineage in both samples. As shown in Figure 21, the recapitulated dynamics of the NSPC lineage is illustrated with the aNSC clusters acting as a point of origin of cells, with cells moving away from the aNSC clusters and towards either NBs or qNSCs. This is in line with recent studies suggestive of aNSCs in the SVZ as having bidirectionality in the NSPC lineage, with them either reverting to a quiescent state or moving to become NBs (Basak et al., 2018). Further, there are no striking differences between the stroke and naïve sample, indicating that the general directionality of the lineage progression does not appear to differ following stroke. Following this observation, analysis was performed to identify if there are any differences in the rate of cells transitioning to the next cell state by determining the velocity length of sequenced cells (La Manno et al., 2018; Bergen et al., 2020) (Fig 22). Overall, we do not observe any striking differences in the directionality or the rate of progress of cells in the naïve and stroke samples.

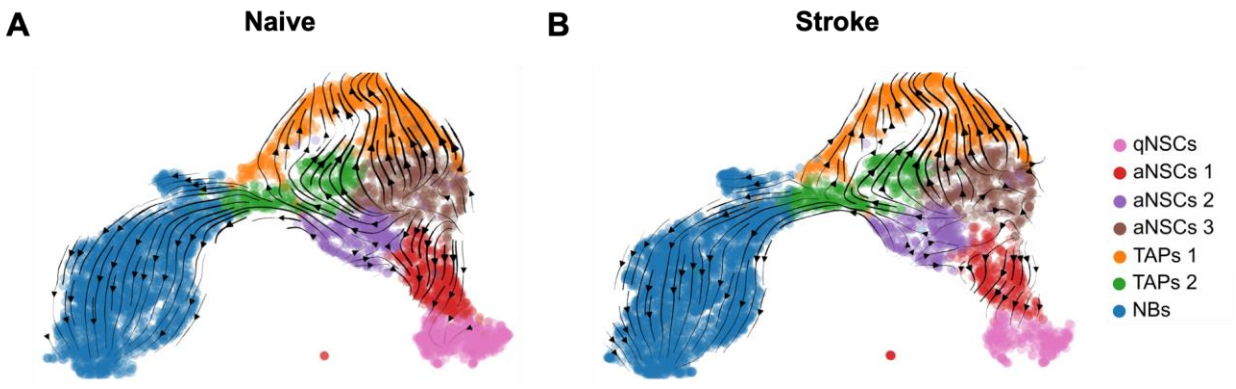


**Figure 21. No differences in RNA projection velocity following stroke.** (A) RNA projection velocity on UMAP embedding of cells isolated from naïve (A) and stroke (B) mice.

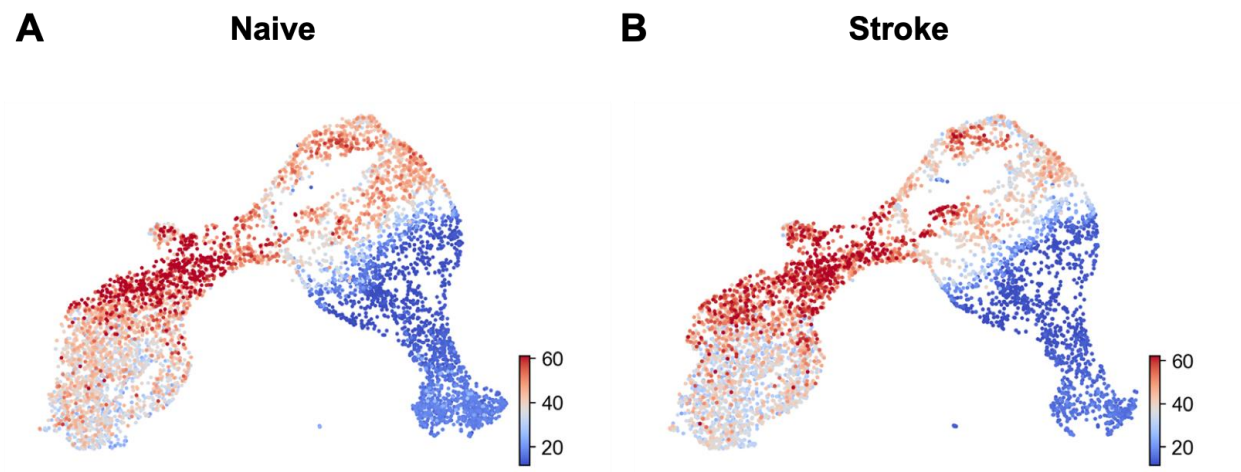


**Figure 22. Stroke does not induce changes in rate of transition of sequenced cells.** Velocity length of sequenced cells isolated from naïve (A) or stroke (B) mice.

### 4.7 Single cell transcriptomics reveals perturbed latent time and velocity of neuronal genes after stroke

To reconstruct the temporal sequence of transcriptome dynamics and cell fates, the latent time, which is a representation of a cell's internal clock and approximates the position of cells differentiating (Bergen et al., 2020), was examined between the naïve and stroke samples (Fig 23). Using latent time, the root cells of the lineage are assigned a latent time value of 0 with cells at the end of the lineage being assigned values closer to 1. Interestingly in both samples the aNSC clusters were identified as a starting point on the latent time continuum, with cells in aNSC 3 appearing as the primarily assigned root cells. This is likely due to the presence of multiple directionalities being observed as deriving from this cell cluster. In the qNSC population it is most notable that the stroke and naïve sample differ in latent time. In the stroke group the qNSCs are farther along the continuum compared to those in the naïve sample. This suggests that the cells in the stroke group either 1) take longer for aNSCs to return to qNSC, or 2) have a decreased probability of returning to qNSCs when compared to the naïve group. Together, this suggests that labelling NSPCs following stroke identifies cells being in a state more likely to move towards a neuronal fate.

As there were differences in cellular transcriptional profiles for neuronal and astrocyte genes, analysis was performed to identify driver genes that are involved in dictating the velocity of cells sequenced. Interestingly, neuronal genes such as DCX were identified as driver genes in our output and as deviating from the steady state ratio (Fig 24). Looking at the RNA velocity of neuronal genes such as DCX and Stmn2 reveals following stroke the velocity for DCX and Stmn2 is more negative across all cell types. The steady state regression analysis was compared between samples to identify what is underlying the differences in velocity observed and at which cell

clusters it is present (Fig 25). Specifically, the slope of the steady state regression analysis for DCX is shorter on the x-axis of the naïve sample relative to the stroke sample in the TAP clusters. This indicates that TAPs in the stroke mice have an increased induction of spliced RNA for DCX and thus that stroke is inducing increased induction of DCX splicing at the stage at which neuronal genes become upregulated in the NSPC lineage (Magnusson et al., 2020). Given the use of RNA velocity relies on looking at the ratio of spliced to unspliced mRNA, we went to validate that the overall and cell-type specific RNA splicing is stable between samples. Upon quantification, the splicing ratio overall appears stable between the naïve and stroke sample, with approximately 68-69% of mRNA in both samples being spliced, and the cell-type specific spliced RNA proportion being appearing stable between samples (Fig 26). Together, these findings suggest that TAPs in the stroke group have an increased induction of spliced RNA for DCX which may be contributing to increased uptake of neuronal fate after stroke.

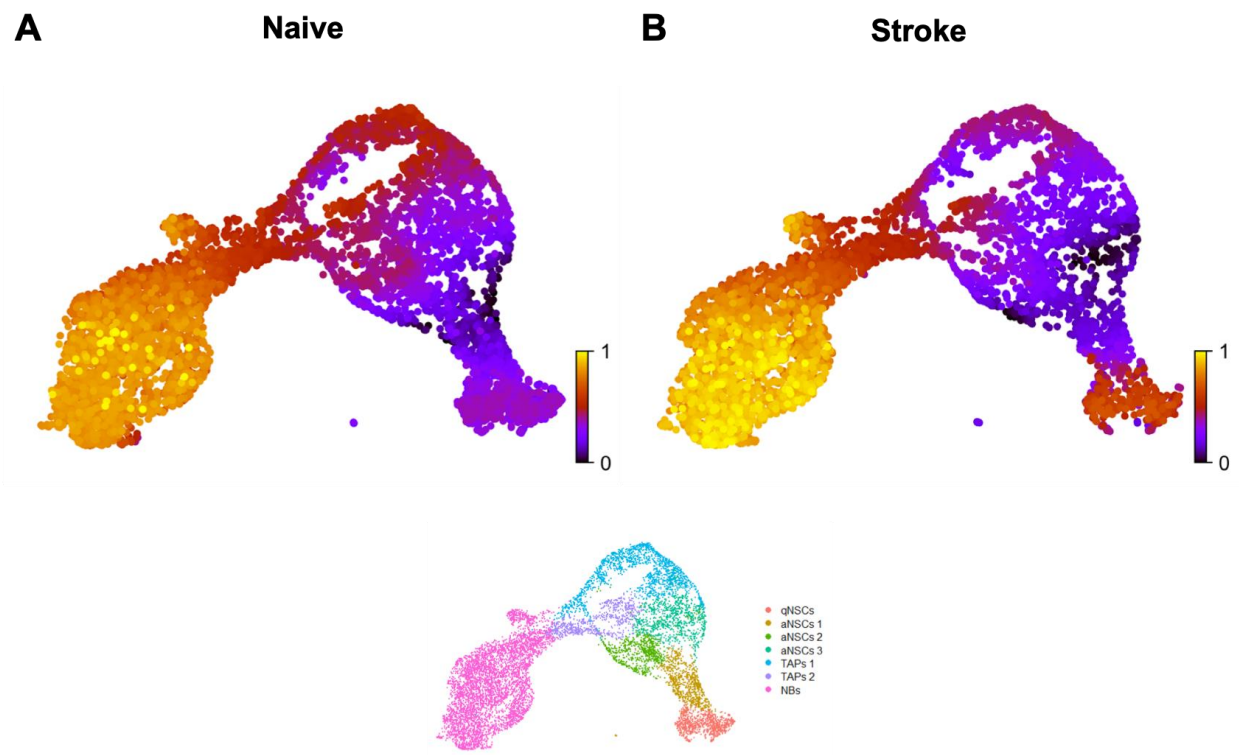


**Figure 23. Stroke induces changes in latent time of cells labelled after stroke.** Latent time of sequenced cells isolated from naïve (A) and stroke (B) mice.

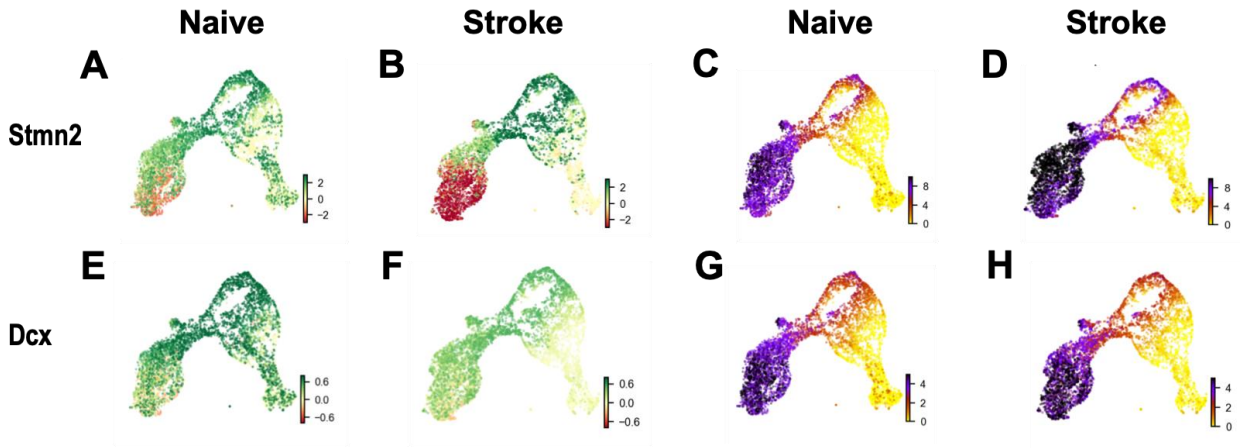


**Figure 24. RNA velocity of neuronal genes is reduced following stroke.** RNA velocity of Stmn2 in naïve (A) and stroke (B) mice. Expression of Stmn2 in naïve (C) and stroke (D) mice. RNA velocity of Dcx in naïve (E) and stroke (F) mice. Expression of Dcx in naïve (G) and stroke (F) mice.

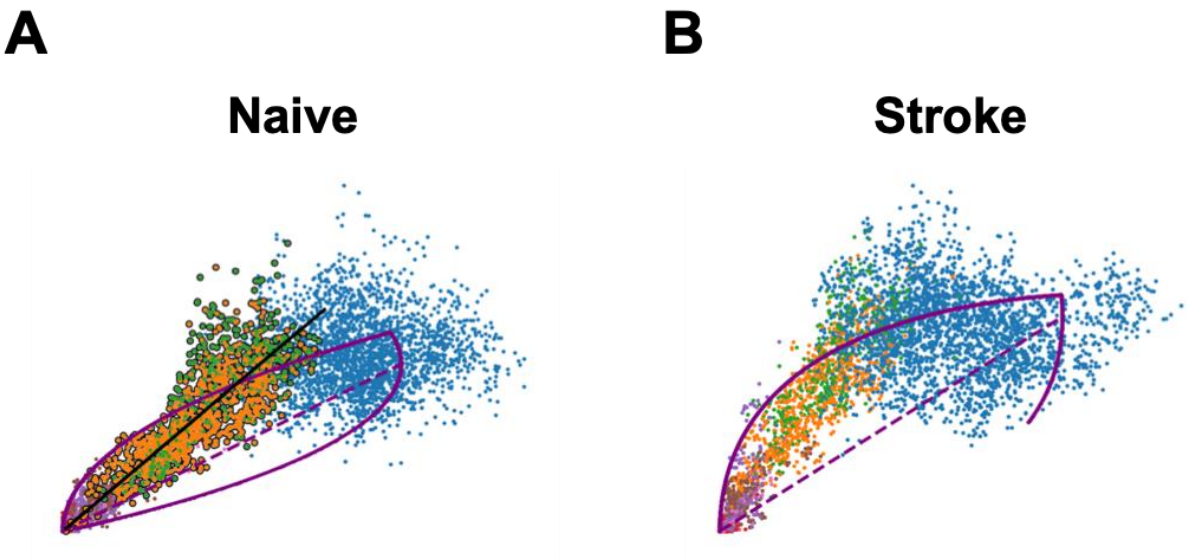


**Figure 25. Stroke induces altered kinetics of Dcx following stroke.** Steady state dynamic regression of Dcx in sequenced cells isolated from naïve (A) and stroke (B) mice.

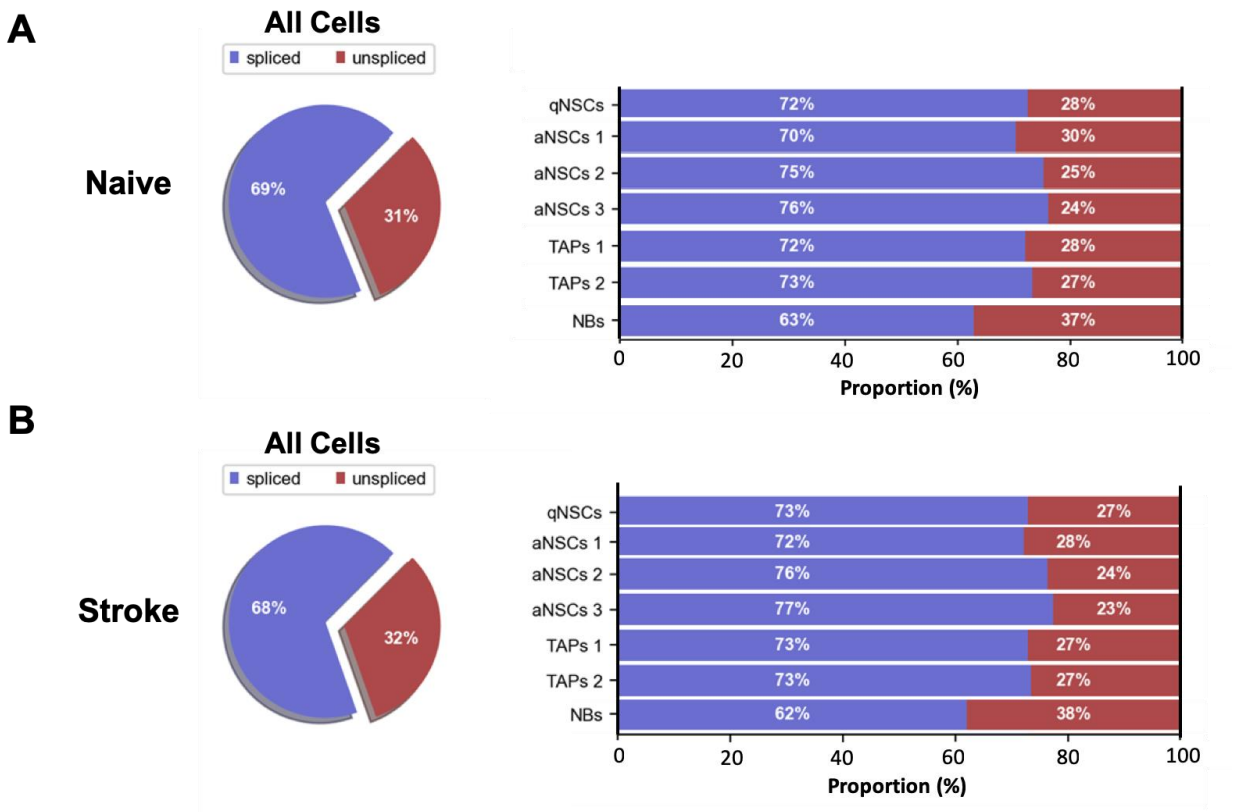


**Figure 26. Stroke does not induce changes to proportions of spliced/unspliced counts across cells sequenced.** Proportion of spliced and unspliced counts across all sequenced cells isolated from naïve (A) and stroke (B) mice.

# 5. Discussion

## 5.1 Summary

The overarching aim of this thesis is to elucidate the profiles of NSPCs being labelled after stroke and the transcriptional modifications occurring after stroke associated with a neuronal fate. Altogether, the work conducted shows that when nestin-expressing NSPCs located in the SVZ are labelled at least 7 days after stroke, the NSPCs are able to produce a majority of neuronal, instead of astrocyte-fated progeny in the peri-infarct area. This temporal difference in fate of the NSPCs did not appear to be due to different populations of cells at the SVZ being labeled after stroke, given that the same population of cells were identified in the absence or presence of a stroke based on scRNAseq analysis. Labeling the NSPCs after stroke did however reduce the proportion of qNSCs, while increasing the number of NBs in the SVZ. Differential gene expression analysis further revealed after stroke the labeled qNSCs and aNSCs had a reduction in astrocytic gene expression, which was accompanied by an enrichment of neuronal genes in all cells labeled. The transcriptional dynamics following stroke further revealed no difference in trajectory or velocity of NSPCs labelled after stroke, while analysis of the latent time of NSPCs labelled after stroke revealed a decreased probability of the labeled NSPCs after stroke returning to a qNSC state. This occurred in tandem with perturbation in transcriptional dynamics of neuronal genes driving the velocity of NSPCs following stroke. Therefore, altogether these data suggest there is an induction of a neuronal fate in the NSPCs found in the SVZ long term after stroke, which likely contributes to generation of the neuronal-fated progeny that arises within the stroke-injured cortex.

### 5.2 SVZ Nestin-Expressing NSPCs Labelled 7 Days After Stroke Produce Neurons

We have shown a long-term neuronal response from progeny of NSPCs labeled at the SVZ after stroke surrounding the infarct. This is in striking contrast to previous findings that have shown a majority of cells that migrate to the peri-infarct region becoming astrocytes, with very few neurons being produced (Li et al., 2010; Benner et al., 2013; Faiz et al., 2015). We hypothesize that the neuronal response differs from previous studies largely due to the labeling of the NSPCs at the SVZ being done prior to induction of stroke. The labelling of NSPCs after stroke was initially performed in our lab due to the rationale that this would allow for labelling of more NSPCs relative to the number typically labelled before stroke (Ceizar, 2017). When examining the temporal specificity of labelling NSPCs fated to become neurons, the data in this thesis shows that labelling the NSPCs in the SVZ with one injection of TAM at 2 or 7 days after stroke resulted with the labeled cells surrounding the infarct at 2 weeks after TAM injection expressing the astrocytic marker GFAP. In contrast, when injecting TAM at 14 days after stroke there was a greater proportion of cells that had migrated by 2 weeks to surround the infarct and express the neuronal marker DCX.

Recent work by Pous et al. (2020), identified that there are temporal changes in the microenvironment that regulate uptake of an astrocytic fate in SVZ-derived NSPCs. Specifically, they observed the coagulation factor fibrinogen deposited in the SVZ and cortex following stroke, with fibrinogen deposition being required to induce signalling via the Id3-BMP axis to promote an astrocyte fate in these cells. In this previous report, they do not assess if the fate of NSPCs changes *in vivo* at timepoints following fibrinogen loss and also do not assess if NSPCs differentiate into neurons at the site of stroke *in vivo*. Our work thus fills the gap left by this previous report as we show NSPCs labelled 2 days post-stroke as differentiating into astrocytes

when fibrinogen is reported to be present, but NSPCs labelled at 14 days post-stroke when fibrinogen is reported to be depleted instead differentiate primarily into neurons at the site of stroke.

There are two other studies that have tracked the fate of NSPCs labelled after stroke that produced results that align with our data. However, both of these studies labeled the NSPCs post stroke, as well as adding on an additional method that is known to stimulate neurogenesis. For example, in one study NSPCs labelled after stroke using BrdU had a neuronal fate, however brain-derived neurotrophic factor (BDNF) was also administered following stroke (Keiner et al., 2009). More recently, fate mapping of NSPCs labelled following stroke using Ascl1 to drive YFP recombination also showed neuronal fated cells (Liang et al., 2019). However, Ascl1 has been shown to promote neuronal differentiation and is upregulated more in TAPs, thus making the labelled cells already predisposed to move towards a neuronal fate (Castro et al., 2011; Liang et al., 2019).

The experiments in this study used the nestinCreER$^{T2}$ mouse combined with the photothrombosis stroke model. To determine if these findings generalize to other models, it will be important for future work to assess if the stroke-induced phenotypes that were found in this study occur when using other models to label NSPCs following stroke, as well as other models to induce a stroke. The advantage of using the nestinCreER$^{T2}$ mouse model used in this study to label and fate-map nestin-expressing NSPCs migrating to the site of injury is that this model has been shown to have specific expression in NSPCs (Lagace et al., 2007; Dranovsky et al., 2011; Sahay et al., 2011). This is in contrast to other nestinCreER$^{T2}$ models that can have substantial expression outside of the neurogenic regions (Sun et al., 2014) or other inducible models such as

GFAP-CreER$^{T2}$ models that can label both SVZ niche astrocytes, as well as the NPSCs. Alongside the findings presented here being specific so far to the nestinCreERT2 mouse model, our results are limited by being tested with the use of the photothrombosis stroke model. This is in contrast to the numerous previous studies that have shown the endogenous astrogenic response occurring when labelling the NSPCs before stroke in a various number of injury models. Thus, future work should test if the neuronal-fated NSPC response is conserved when labelling NSPCs after other cortical injuries, and with other transgenic reporter lines. Given the presence of established similarities between stroke and other injury models such as traumatic brain injury, there is potential that the neuronal-fated NSPC response is an endogenous mechanism of the brain that occurs after all forms of brain injury.

### 5.3 Insights Gained from scRNAseq Analysis of SVZ Cells Labeled Post Stroke

Single-cell RNA sequencing techniques have vastly improved the capacity of lineage tracing to decipher progenitor potential (Figueres-Oñate et al., 2020), thus this thesis used scRNAseq to examine the difference in cells labeled at the SVZ before or after stroke, as well as their lineage. One hypothesis could be that the neuronal-fated NSPCs labeled after stroke and localizing at the site of injury are due to a new population of NSPCs being labeled that had nestin-expression induced in them post-stroke. In support of this hypothesis the induction of a stroke is associated with an increase in the number of nestin+ cells in the SVZ (Krishnasamy et al., 2017). It also remains unreported if all NSPCs hold the same potential in differentiating into neurons vs. glial cells under naïve conditions (Chaker et al., 2016). However, in contrast to this hypothesis the scRNAseq dataset revealed no difference in the types of NSPCs labelled in the absence and

presence of a stroke. This finding therefore suggests that the potential of the NSPCs to become neurons when labeled after stroke is not due to a different population of cells being labeled.

One of the differences revealed by scRNAseq in the stroke sample was a reduction in the proportion of qNSCs and increase in proportion of NBs. These findings were found through analysis of the scRNAseq dataset, as well as confirmed using immunohistochemical analysis of cells in the SVZ. The reduction of qNSCs is in agreement with previous work by Llorens-Bobadilla et al. (2015) who looked at the injury-induced changes present in the SVZ following a transient bilateral common carotid artery occlusion. Specifically, they observed using scRNAseq following injury a shift of two qNSC subpopulations towards activation, leading to a smaller proportion of qNSCs in the SVZ. In line with these findings, the qNSC cluster we identify had a transcriptional profile similar to the qNSCs 1 cluster presented in this previous study. Although we observe a reduced proportion of qNSCs present following stroke, future work should assess if changes in NSPC activation contribute to neuronal fate uptake.

Given our previous work labelling NSPCs after stroke showing reduced proportions of astrocyte-fated NSPCs at the site of injury, it may seem surprising that the analysis did not identify any clusters indicative of astrocyte-fated NSPCs in the scRNAseq dataset. One hypothesis that could explain why we do not see cells that are differentiating into astrocytes is because they are within the qNSCs cluster. In general, there is a lack of consensus in being able to separate qNSC and astrocytes in scRNAseq datasets, even with the unprecedented resolution that scRNAseq provides (Dulken et al., 2017; Dulken et al., 2019; Kalamakis et al., 2019). To this end, previous reports have often defined their clusters as “qNSC/Astrocytes” due to being unable to discriminate between the two types of cells (Dulken et al., 2019). We find markers for astrocytes

are enriched in the qNSC cluster, such that if there are cells differentiating into astrocytes within the SVZ, they are not forming their own cluster due to having very similar transcriptomic profiles to SVZ-derived qNSCs. Since the stroke sample has a smaller proportion of qNSCs, one interpretation of this data could suggest that following stroke less astrocytes are being produced. If correct, this would support our finding that following stroke there is a shift to producing neurons fated for the site of injury. This could be tested in future experiments by immunohistochemical characterization of YFP+ GFAP+ cells in the SVZ alongside a marker of quiescence such as Id2 to see if YFP+ astrocytes at the SVZ are expressing markers of qNSCs.

Analysis of cell dynamics by use of RNA velocity further showed that in both the control and stroke sample that the aNSCs had a profile that suggested that they could revert to quiescence (Fig 21). This is in line with reports of maintenance of the qNSC population through aNSCs reverting to quiescence (Basak et al., 2018; Obernier et al., 2018). Basak et al. (2018) validate this model by use of a Ki67iresCreER mouse model that labels dividing cells, such that they observed dividing cells in the SVZ returning to quiescence over time. Our findings compliment this report and provide further evidence of the self-regulation of the NSPC pool present in adult mice. This finding also leads to the interesting question about the extent to which stroke-induced cell division contributes to the state of the NSPC lineage, as suggested to occur by Basak et al. (2018). Although changes in composition of the SVZ can be suggested to affect the degree of activation and quiescence observed by NSPCs, it is not reported if such changes can alter the differentiation of cells into neurons and astrocytes under naïve or stroke conditions.

Given the presence of self-regulation of the NSPC pool in both samples reported, it was of interest to look if there were any differences in the extent of self-regulation present after

stroke by analysing the latent time of cells. As shown in Figure 23, we observe the aNSC clusters as the root cells on the latent time continuum with NBs at the end of the continuum in the naïve sample. In contrast, in the stroke sample the aNSC cluster is the root, but both the NB and the qNSC clusters are placed on the end of the continuum. This difference in positioning of qNSCs on the continuum for the stroke sample is suggestive that stroke can reduce the probability of aNSCs returning to becoming qNSCs. Given the association of changes in quiescence reported in this thesis after stroke with increased uptake of neuronal fate, it is of interest to test if changes in the proportion of qNSCs shown to occur, in line with changes in regulation of the NSPC pool in the SVZ, could be sufficient to contribute to NSPC fate changes after stroke.

### 5.4 Future Questions and Implications of Adult-Generated Neurons Post-Stroke

Future work should investigate the type of neurons being produced and function of the neuronal-fated NSPC response labelled after injury. Analysis of the scRNAseq dataset suggests that the labelled NSPCs migrating towards the site of injury express markers of periglomerular neurons, which has yet to be validated by immunohistochemical characterization. This is in line with previous reports from our lab suggesting that the adult-born neurons at the site of injury have functional features of periglomerular neurons found in the adult OB, including being able to fire action potentials, alongside being hyper-excitable and receiving primarily GABAergic synaptic inputs (Kannangara et al., 2018). This is in contrast to previous reports that theorized stroke-induced neurons are of subtypes typically found in the brain regions where the cells localize (Arvidsson et al., 2002; Parent et al., 2002). Furthermore, the notion that there are neurons migrating to the site of injury provides evidence towards the possibility that the NSPCs migrating to the site of injury are in fact NSPCs that are re-routing from the RMS (Kannangara et

al., 2018). Pous et al. (2020) suggest that the fibrinogen deposition present following stroke is sufficient to drive production of astrocytes fated to the site of injury at the expense of OB neurogenesis. Future work should thus assess if the neuronal-fated NSPC response reported in this thesis is also occurring at the expense of OB neurogenesis.

Given our results show that there are stroke-induced neurons at the site of injury following stroke, it is important to consider the functional role of these cells in stroke recovery as the purpose of this work is to enhance recovery. Numerous studies have suggested that increasing neurogenesis can improve recovery, however most of this work is limited to correlative evidence that show correlations between increase neurogenesis and improving function (Lagace, 2012). Our lab has tried to overcome these limitations to specifically address if increasing the number of neurons surrounding the injury is sufficient to promote recovery. Maheen Ceizar in our lab assessed the functional role of enhancing progenitor cell survival following stroke using the nestinCreER$^{T2}$ iBax transgenic mouse, which increased NSPC survival through conditional knockout of Bax, a key regulator of apoptosis (Sahay et al., 2011; Ceizar, 2017). The iBax mouse had a dramatic enhancement in the number of adult-born neurons that survived following stroke yet did not result in any improvements in behavioral recovery. These findings suggest that increasing the survival of the NSPCs and development of new neurons in the cortex is not sufficient to improve recovery. We had also shown in a nestin-GFP reporter mouse that although the cells can have a neuronal phenotype surrounding the infarct post stroke, they are sparsely innervated (Kannangara et al., 2018). This led us to hypothesize that the cells may not have been able to improve recovery due to the cells having inadequate innervation. However, work by our lab used optogentics to stimulate the adult-born neurons at the site of injury, yet this also did

not result in any change in recovery post stroke (Denize, 2020). Although all of these studies have limitations, it has been disappointing to observe that enhancing the number or activity of adult-generated neurons following stroke is insufficient to improve recovery.

Interesting recent work by others has been more supportive of the role of adult-generated neurons in promoting recovery. For example, use of tetanus toxin to silence migrated neurons revealed a reduction in functional recovery following stroke (Liang et al., 2019). This finding suggested there is a specific requirement of proper synaptic function from SVZ-derived neurons in stroke recovery. However, they also raise the question about whether a gain of synaptic function in this population enhances stroke recovery. Together, these findings highlight the potential of neurogenesis in improving recovery after stroke, with our lab working towards elucidating how to harness the neuronal-fated NSPC response following stroke.

**5.5 Concluding Remarks**

Given the tremendously successful efforts in improving patient survival following stroke, there is a clear need to find ways to improve upon the long-term deficits endured by stroke survivors. There are currently numerous studies aimed at using exogenous treatments to improve recovery, albeit there being many hurdles present in this pursuit, such as stem cell transplants that can be rejected by the recipient and non-invasive stimulation of the brain lacking specificity. Instead of exogenous treatments that come with such complications, our lab is working to harness the endogenous mechanisms already present in the brain to improve recovery. Altogether the findings presented in this thesis change the perspective regarding the post-stroke NSPC response, with us thus raising the challenge of now determining how to best harness this response to improve stroke recovery.

# 6. References


Arvidsson A, Collin T, Kirik D, Kokaia Z, Lindvall O (2002) Neuronal replacement from endogenous precursors in the adult brain after stroke. Nat Med 8:963-970.

Ashburner M, Ball CA, Blake JA, Botstein D, Butler H, Cherry JM, Davis AP, Dolinski K, Dwight SS, Eppig JT, Harris MA, Hill DP, Issel-Tarver L, Kasarskis A, Lewis S, Matese JC, Richardson JE, Ringwald M, Rubin GM, Sherlock G (2000) Gene ontology: tool for the unification of biology. The Gene Ontology Consortium. Nat Genet 25:25-29.

Barkho BZ, Munoz AE, Li X, Li L, Cunningham LA, Zhao X (2008) Endogenous matrix metalloproteinase (MMP)-3 and MMP-9 promote the differentiation and migration of adult neural progenitor cells in response to chemokines. Stem Cells 26:3139-3149.

Basak O, Krieger TG, Muraro MJ, Wiebrands K, Stange DE, Frias-Aldeguer J, Rivron NC, van de Wetering M, van Es JH, van Oudenaarden A, Simons BD, Clevers H (2018) Troy+ brain stem cells cycle through quiescence and regulate their number by sensing niche occupancy. Proc Natl Acad Sci U S A 115:E610-E619.

Beck H, Plate KH (2009) Angiogenesis after cerebral ischemia. Acta Neuropathol 117:481-496.

Benner EJ, Luciano D, Jo R, Abdi K, Paez-Gonzalez P, Sheng H, Warner DS, Liu C, Eroglu C, Kuo CT (2013) Protective astrogenesis from the SVZ niche after injury is controlled by Notch modulator Thbs4. Nature 497:369-373.

Bergen V, Lange M, Peidli S, Wolf FA, Theis FJ (2020) Generalizing RNA velocity to transient cell states through dynamical modeling. Nat Biotechnol.

Bergmann O, Spalding KL, Frisén J (2015) Adult Neurogenesis in Humans. Cold Spring Harb Perspect Biol 7:a018994.

Boldrini M, Fulmore CA, Tartt AN, Simeon LR, Pavlova I, Poposka V, Rosoklija GB, Stankov A, Arango V, Dwork AJ, Hen R, Mann JJ (2018) Human Hippocampal Neurogenesis Persists throughout Aging. Cell Stem Cell 22:589-599.e585.

Bond AM, Ming GL, Song H (2015) Adult Mammalian Neural Stem Cells and Neurogenesis: Five Decades Later. Cell Stem Cell 17:385-395.

Brown JP, Couillard-Després S, Cooper-Kuhn CM, Winkler J, Aigner L, Kuhn HG (2003) Transient expression of doublecortin during adult neurogenesis. J Comp Neurol 467:1-10.

Cassidy JM, Cramer SC (2017) Spontaneous and Therapeutic-Induced Mechanisms of Functional Recovery After Stroke. Transl Stroke Res 8:33-46.

Castro DS, Martynoga B, Parras C, Ramesh V, Pacary E, Johnston C, Drechsel D, Lebel-Potter M, Garcia LG, Hunt C, Dolle D, Bithell A, Ettwiller L, Buckley N, Guillemot F (2011) A novel function of the proneural factor Ascl1 in progenitor proliferation identified by genome-wide characterization of its targets. Genes Dev 25:930-945.

Ceizar M (2017) Evaluating the Functional Role of Enhancing Progenitor Cell Survival Following Stroke Recovery. In: Cellular and Molecular Medicine, p 225: University of Ottawa.

Chaker Z, Codega P, Doetsch F (2016) A mosaic world: puzzles revealed by adult neural stem cell heterogeneity. Wiley Interdiscip Rev Dev Biol 5:640-658.

Codega P, Silva-Vargas V, Paul A, Maldonado-Soto AR, Deleo AM, Pastrana E, Doetsch F (2014) Prospective identification and purification of quiescent adult neural stem cells from their in vivo niche. Neuron 82:545-559.

Cramer SC (2008) Repairing the human brain after stroke: I. Mechanisms of spontaneous recovery. Ann Neurol 63:272-287.
Denize S (2020) The Functional Role of Enhancing the Survival and Activity of Progenitor Cells During Stroke Recovery. In: Neuroscience: University of Ottawa.
Dranovsky A, Picchini AM, Moadel T, Sisti AC, Yamada A, Kimura S, Leonardo ED, Hen R (2011) Experience dictates stem cell fate in the adult hippocampus. Neuron 70:908-923.
Dulken BW, Leeman DS, Boutet SC, Hebestreit K, Brunet A (2017) Single-Cell Transcriptomic Analysis Defines Heterogeneity and Transcriptional Dynamics in the Adult Neural Stem Cell Lineage. Cell Rep 18:777-790.
Dulken BW, Buckley MT, Navarro Negredo P, Saligrama N, Cayrol R, Leeman DS, George BM, Boutet SC, Hebestreit K, Pluvinage JV, Wyss-Coray T, Weissman IL, Vogel H, Davis MM, Brunet A (2019) Single-cell analysis reveals T cell infiltration in old neurogenic niches. Nature 571:205-210.
Ergul A, Alhusban A, Fagan SC (2012) Angiogenesis: a harmonized target for recovery after stroke. Stroke 43:2270-2274.
Eriksson PS, Perfilieva E, Björk-Eriksson T, Alborn AM, Nordborg C, Peterson DA, Gage FH (1998) Neurogenesis in the adult human hippocampus. Nat Med 4:1313-1317.
Faiz M, Sachewsky N, Gascón S, Bang KW, Morshead CM, Nagy A (2015) Adult Neural Stem Cells from the Subventricular Zone Give Rise to Reactive Astrocytes in the Cortex after Stroke. Cell Stem Cell 17:624-634.
Figueres-Oñate M, Sánchez-González R, López-Mascaraque L (2020) Deciphering neural heterogeneity through cell lineage tracing. Cell Mol Life Sci.
Fisher M (2010) The challenge of mixed cerebrovascular disease. Ann N Y Acad Sci 1207:18-22.
Gertz K, Priller J, Kronenberg G, Fink KB, Winter B, Schröck H, Ji S, Milosevic M, Harms C, Böhm M, Dirnagl U, Laufs U, Endres M (2006) Physical activity improves long-term stroke outcome via endothelial nitric oxide synthase-dependent augmentation of neovascularization and cerebral blood flow. Circ Res 99:1132-1140.
Grefkes C, Ward NS (2014) Cortical reorganization after stroke: how much and how functional? Neuroscientist 20:56-70.
Hayashi T, Noshita N, Sugawara T, Chan PH (2003) Temporal profile of angiogenesis and expression of related genes in the brain after ischemia. J Cereb Blood Flow Metab 23:166-180.
Imitola J, Raddassi K, Park KI, Mueller FJ, Nieto M, Teng YD, Frenkel D, Li J, Sidman RL, Walsh CA, Snyder EY, Khoury SJ (2004) Directed migration of neural stem cells to sites of CNS injury by the stromal cell-derived factor 1alpha/CXC chemokine receptor 4 pathway. Proc Natl Acad Sci U S A 101:18117-18122.
Iosif RE, Ahlenius H, Ekdahl CT, Darsalia V, Thored P, Jovinge S, Kokaia Z, Lindvall O (2008) Suppression of stroke-induced progenitor proliferation in adult subventricular zone by tumor necrosis factor receptor 1. J Cereb Blood Flow Metab 28:1574-1587.
Janky R, Verfaillie A, Imrichová H, Van de Sande B, Standaert L, Christiaens V, Hulselmans G, Herten K, Naval Sanchez M, Potier D, Svetlichnyy D, Kalender Atak Z, Fiers M, Marine JC, Aerts S (2014) iRegulon: from a gene list to a gene regulatory network using large motif and track collections. PLoS Comput Biol 10:e1003731.

Ji JF, He BP, Dheen ST, Tay SS (2004) Expression of chemokine receptors CXCR4, CCR2, CCR5 and CX3CR1 in neural progenitor cells isolated from the subventricular zone of the adult rat brain. Neurosci Lett 355:236-240.

Jin K, Wang X, Xie L, Mao XO, Zhu W, Wang Y, Shen J, Mao Y, Banwait S, Greenberg DA (2006) Evidence for stroke-induced neurogenesis in the human brain. Proc Natl Acad Sci U S A 103:13198-13202.

Kalamakis G et al. (2019) Quiescence Modulates Stem Cell Maintenance and Regenerative Capacity in the Aging Brain. Cell 176:1407-1419.e1414.

Kannangara TS, Carter A, Xue Y, Dhaliwal JS, Béïque JC, Lagace DC (2018) Excitable Adult-Generated GABAergic Neurons Acquire Functional Innervation in the Cortex after Stroke. Stem Cell Reports 11:1327-1336.

Keiner S, Witte OW, Redecker C (2009) Immunocytochemical detection of newly generated neurons in the perilesional area of cortical infarcts after intraventricular application of brain-derived neurotrophic factor. J Neuropathol Exp Neurol 68:83-93.

Kempermann G, Gage FH, Aigner L, Song H, Curtis MA, Thuret S, Kuhn HG, Jessberger S, Frankland PW, Cameron HA, Gould E, Hen R, Abrous DN, Toni N, Schinder AF, Zhao X, Lucassen PJ, Frisén J (2018) Human Adult Neurogenesis: Evidence and Remaining Questions. Cell Stem Cell 23:25-30.

Kim GH, Mocco J, Hahn DK, Kellner CP, Komotar RJ, Ducruet AF, Mack WJ, Connolly ES (2008) Protective effect of C5a receptor inhibition after murine reperfused stroke. Neurosurgery 63:122-125; discussion 125-126.

Kohwi M, Osumi N, Rubenstein JL, Alvarez-Buylla A (2005) Pax6 is required for making specific subpopulations of granule and periglomerular neurons in the olfactory bulb. J Neurosci 25:6997-7003.

Kojima T, Hirota Y, Ema M, Takahashi S, Miyoshi I, Okano H, Sawamoto K (2010) Subventricular zone-derived neural progenitor cells migrate along a blood vessel scaffold toward the post-stroke striatum. Stem Cells 28:545-554.

Krishnasamy S, Weng YC, Thammisetty SS, Phaneuf D, Lalancette-Hebert M, Kriz J (2017) Molecular imaging of nestin in neuroinflammatory conditions reveals marked signal induction in activated microglia. J Neuroinflammation 14:45.

La Manno G et al. (2018) RNA velocity of single cells. Nature 560:494-498.

Lagace DC (2012) Does the endogenous neurogenic response alter behavioral recovery following stroke? Behav Brain Res 227:426-432.

Lagace DC, Whitman MC, Noonan MA, Ables JL, DeCarolis NA, Arguello AA, Donovan MH, Fischer SJ, Farnbauch LA, Beech RD, DiLeone RJ, Greer CA, Mandyam CD, Eisch AJ (2007) Dynamic contribution of nestin-expressing stem cells to adult neurogenesis. J Neurosci 27:12623-12629.

Langhorne P, Bernhardt J, Kwakkel G (2011) Stroke rehabilitation. Lancet 377:1693-1702.

Li L, Harms KM, Ventura PB, Lagace DC, Eisch AJ, Cunningham LA (2010) Focal cerebral ischemia induces a multilineage cytogenic response from adult subventricular zone that is predominantly gliogenic. Glia 58:1610-1619.

Li WL, Chu MW, Wu A, Suzuki Y, Imayoshi I, Komiyama T (2018) Adult-born neurons facilitate olfactory bulb pattern separation during task engagement. Elife 7.

Liang H, Zhao H, Gleichman A, Machnicki M, Telang S, Tang S, Rshtouni M, Ruddell J, Carmichael ST (2019) Region-specific and activity-dependent regulation of SVZ neurogenesis and recovery after stroke. Proc Natl Acad Sci U S A 116:13621-13630.
Lim DA, Alvarez-Buylla A (2016) The Adult Ventricular-Subventricular Zone (V-SVZ) and Olfactory Bulb (OB) Neurogenesis. Cold Spring Harb Perspect Biol 8.
Lindvall O, Kokaia Z (2015) Neurogenesis following Stroke Affecting the Adult Brain. Cold Spring Harb Perspect Biol 7.
Liu K, Liu Y, Mo W, Qiu R, Wang X, Wu JY, He R (2011) MiR-124 regulates early neurogenesis in the optic vesicle and forebrain, targeting NeuroD1. Nucleic Acids Res 39:2869-2879.
Liu XS, Chopp M, Wang XL, Zhang L, Hozeska-Solgot A, Tang T, Kassis H, Zhang RL, Chen C, Xu J, Zhang ZG (2013) MicroRNA-17-92 cluster mediates the proliferation and survival of neural progenitor cells after stroke. J Biol Chem 288:12478-12488.
Llorens-Bobadilla E, Zhao S, Baser A, Saiz-Castro G, Zwadlo K, Martin-Villalba A (2015) Single-Cell Transcriptomics Reveals a Population of Dormant Neural Stem Cells that Become Activated upon Brain Injury. Cell Stem Cell 17:329-340.
Lu PP, Ramanan N (2012) A critical cell-intrinsic role for serum response factor in glial specification in the CNS. J Neurosci 32:8012-8023.
López-Juárez A, Howard J, Ullom K, Howard L, Grande A, Pardo A, Waclaw R, Sun YY, Yang D, Kuan CY, Campbell K, Nakafuku M (2013) Gsx2 controls region-specific activation of neural stem cells and injury-induced neurogenesis in the adult subventricular zone. Genes Dev 27:1272-1287.
Macas J, Nern C, Plate KH, Momma S (2006) Increased generation of neuronal progenitors after ischemic injury in the aged adult human forebrain. J Neurosci 26:13114-13119.
Magnusson JP, Zamboni M, Santopolo G, Mold JE, Barrientos-Somarribas M, Talavera-Lopez C, Andersson B, Frisén J (2020) Activation of a neural stem cell transcriptional program in parenchymal astrocytes. Elife 9.
Marlier Q, Verteneuil S, Vandenbosch R, Malgrange B (2015) Mechanisms and Functional Significance of Stroke-Induced Neurogenesis. Front Neurosci 9:458.
Martí-Fàbregas J, Romaguera-Ros M, Gómez-Pinedo U, Martínez-Ramírez S, Jiménez-Xarrié E, Marín R, Martí-Vilalta JL, García-Verdugo JM (2010) Proliferation in the human ipsilateral subventricular zone after ischemic stroke. Neurology 74:357-365.
Meller R, Stevens SL, Minami M, Cameron JA, King S, Rosenzweig H, Doyle K, Lessov NS, Simon RP, Stenzel-Poore MP (2005) Neuroprotection by osteopontin in stroke. J Cereb Blood Flow Metab 25:217-225.
Menn B, Garcia-Verdugo JM, Yaschine C, Gonzalez-Perez O, Rowitch D, Alvarez-Buylla A (2006) Origin of oligodendrocytes in the subventricular zone of the adult brain. J Neurosci 26:7907-7918.
Merkle FT, Mirzadeh Z, Alvarez-Buylla A (2007) Mosaic organization of neural stem cells in the adult brain. Science 317:381-384.
Mi H, Muruganujan A, Ebert D, Huang X, Thomas PD (2019) PANTHER version 14: more genomes, a new PANTHER GO-slim and improvements in enrichment analysis tools. Nucleic Acids Res 47:D419-D426.
Miller FD, Gauthier-Fisher A (2009) Home at last: neural stem cell niches defined. Cell Stem Cell 4:507-510.

Moraga A, Pradillo JM, Cuartero MI, Hernández-Jiménez M, Oses M, Moro MA, Lizasoain I (2014) Toll-like receptor 4 modulates cell migration and cortical neurogenesis after focal cerebral ischemia. FASEB J 28:4710-4718.

Moreno-Jiménez EP, Flor-García M, Terreros-Roncal J, Rábano A, Cafini F, Pallas-Bazarra N, Ávila J, Llorens-Martín M (2019) Adult hippocampal neurogenesis is abundant in neurologically healthy subjects and drops sharply in patients with Alzheimer's disease. Nat Med 25:554-560.

Morizur L, Chicheportiche A, Gauthier LR, Daynac M, Boussin FD, Mouthon MA (2018) Distinct Molecular Signatures of Quiescent and Activated Adult Neural Stem Cells Reveal Specific Interactions with Their Microenvironment. Stem Cell Reports 11:565-577.

Murphy TH, Corbett D (2009) Plasticity during stroke recovery: from synapse to behaviour. Nat Rev Neurosci 10:861-872.

Obernier K, Cebrian-Silla A, Thomson M, Parraguez JI, Anderson R, Guinto C, Rodas Rodriguez J, Garcia-Verdugo JM, Alvarez-Buylla A (2018) Adult Neurogenesis Is Sustained by Symmetric Self-Renewal and Differentiation. Cell Stem Cell 22:221-234.e228.

Ohab JJ, Carmichael ST (2008) Poststroke neurogenesis: emerging principles of migration and localization of immature neurons. Neuroscientist 14:369-380.

Ohab JJ, Fleming S, Blesch A, Carmichael ST (2006) A neurovascular niche for neurogenesis after stroke. J Neurosci 26:13007-13016.

Palma-Tortosa S, García-Culebras A, Moraga A, Hurtado O, Perez-Ruiz A, Durán-Laforet V, Parra J, Cuartero MI, Pradillo JM, Moro MA, Lizasoain I (2017) Specific Features of SVZ Neurogenesis After Cortical Ischemia: a Longitudinal Study. Sci Rep 7:16343.

Parent JM, Vexler ZS, Gong C, Derugin N, Ferriero DM (2002) Rat forebrain neurogenesis and striatal neuron replacement after focal stroke. Ann Neurol 52:802-813.

Petersen MA, Ryu JK, Akassoglou K (2018) Fibrinogen in neurological diseases: mechanisms, imaging and therapeutics. Nat Rev Neurosci 19:283-301.

Plate KH, Beck H, Danner S, Allegrini PR, Wiessner C (1999) Cell type specific upregulation of vascular endothelial growth factor in an MCA-occlusion model of cerebral infarct. J Neuropathol Exp Neurol 58:654-666.

Pous L, Deshpande SS, Nath S, Mezey S, Malik SC, Schildge S, Bohrer C, Topp K, Pfeifer D, Fernández-Klett F, Doostkam S, Galanakis DK, Taylor V, Akassoglou K, Schachtrup C (2020) Fibrinogen induces neural stem cell differentiation into astrocytes in the subventricular zone via BMP signaling. Nat Commun 11:630.

Qiu X, Hill A, Packer J, Lin D, Ma YA, Trapnell C (2017a) Single-cell mRNA quantification and differential analysis with Census. Nat Methods 14:309-315.

Qiu X, Mao Q, Tang Y, Wang L, Chawla R, Pliner HA, Trapnell C (2017b) Reversed graph embedding resolves complex single-cell trajectories. Nat Methods 14:979-982.

Rousselot P, Lois C, Alvarez-Buylla A (1995) Embryonic (PSA) N-CAM reveals chains of migrating neuroblasts between the lateral ventricle and the olfactory bulb of adult mice. J Comp Neurol 351:51-61.

Sahay A, Scobie KN, Hill AS, O'Carroll CM, Kheirbek MA, Burghardt NS, Fenton AA, Dranovsky A, Hen R (2011) Increasing adult hippocampal neurogenesis is sufficient to improve pattern separation. Nature 472:466-470.

Sakamoto M, Imayoshi I, Ohtsuka T, Yamaguchi M, Mori K, Kageyama R (2011) Continuous neurogenesis in the adult forebrain is required for innate olfactory responses. Proc Natl Acad Sci U S A 108:8479-8484.

Sarli G, Benazzi C, Preziosi R, Marcato PS (1994) Proliferative activity assessed by anti-PCNA and Ki67 monoclonal antibodies in canine testicular tumours. J Comp Pathol 110:357-368.

Shah PT, Stratton JA, Stykel MG, Abbasi S, Sharma S, Mayr KA, Koblinger K, Whelan PJ, Biernaskie J (2018) Single-Cell Transcriptomics and Fate Mapping of Ependymal Cells Reveals an Absence of Neural Stem Cell Function. Cell 173:1045-1057.e1049.

Sorrells SF, Paredes MF, Cebrian-Silla A, Sandoval K, Qi D, Kelley KW, James D, Mayer S, Chang J, Auguste KI, Chang EF, Gutierrez AJ, Kriegstein AR, Mathern GW, Oldham MC, Huang EJ, Garcia-Verdugo JM, Yang Z, Alvarez-Buylla A (2018) Human hippocampal neurogenesis drops sharply in children to undetectable levels in adults. Nature 555:377-381.

Stuart T, Butler A, Hoffman P, Hafemeister C, Papalexi E, Mauck WM, Hao Y, Stoeckius M, Smibert P, Satija R (2019) Comprehensive Integration of Single-Cell Data. Cell 177:1888-1902.e1821.

Sun MY, Yetman MJ, Lee TC, Chen Y, Jankowsky JL (2014) Specificity and efficiency of reporter expression in adult neural progenitors vary substantially among nestin-CreER(T2) lines. J Comp Neurol 522:1191-1208.

The Gene Ontology Consortium (2019) The Gene Ontology Resource: 20 years and still GOing strong. Nucleic Acids Res 47:D330-D338.

Thored P, Wood J, Arvidsson A, Cammenga J, Kokaia Z, Lindvall O (2007) Long-term neuroblast migration along blood vessels in an area with transient angiogenesis and increased vascularization after stroke. Stroke 38:3032-3039.

Thored P, Arvidsson A, Cacci E, Ahlenius H, Kallur T, Darsalia V, Ekdahl CT, Kokaia Z, Lindvall O (2006) Persistent production of neurons from adult brain stem cells during recovery after stroke. Stem Cells 24:739-747.

Trapnell C, Cacchiarelli D, Grimsby J, Pokharel P, Li S, Morse M, Lennon NJ, Livak KJ, Mikkelsen TS, Rinn JL (2014) The dynamics and regulators of cell fate decisions are revealed by pseudotemporal ordering of single cells. Nat Biotechnol 32:381-386.

Wang X, Mao X, Xie L, Greenberg DA, Jin K (2009) Involvement of Notch1 signaling in neurogenesis in the subventricular zone of normal and ischemic rat brain in vivo. J Cereb Blood Flow Metab 29:1644-1654.

Wang Y, Jin K, Mao XO, Xie L, Banwait S, Marti HH, Greenberg DA (2007) VEGF-overexpressing transgenic mice show enhanced post-ischemic neurogenesis and neuromigration. J Neurosci Res 85:740-747.

Wein T et al. (2018) Canadian stroke best practice recommendations: Secondary prevention of stroke, sixth edition practice guidelines, update 2017. Int J Stroke 13:420-443.

Yamashita T, Ninomiya M, Hernández Acosta P, García-Verdugo JM, Sunabori T, Sakaguchi M, Adachi K, Kojima T, Hirota Y, Kawase T, Araki N, Abe K, Okano H, Sawamoto K (2006) Subventricular zone-derived neuroblasts migrate and differentiate into mature neurons in the post-stroke adult striatum. J Neurosci 26:6627-6636.

Yan YP, Lang BT, Vemuganti R, Dempsey RJ (2009) Osteopontin is a mediator of the lateral migration of neuroblasts from the subventricular zone after focal cerebral ischemia. Neurochem Int 55:826-832.

Yan YP, Sailor KA, Lang BT, Park SW, Vemuganti R, Dempsey RJ (2007) Monocyte chemoattractant protein-1 plays a critical role in neuroblast migration after focal cerebral ischemia. J Cereb Blood Flow Metab 27:1213-1224.

Zhang H, Vutskits L, Pepper MS, Kiss JZ (2003) VEGF is a chemoattractant for FGF-2-stimulated neural progenitors. J Cell Biol 163:1375-1384.

Zhang R, Zhang Z, Wang L, Wang Y, Gousev A, Zhang L, Ho KL, Morshead C, Chopp M (2004) Activated neural stem cells contribute to stroke-induced neurogenesis and neuroblast migration toward the infarct boundary in adult rats. J Cereb Blood Flow Metab 24:441-448.

Zywitza V, Misios A, Bunatyan L, Willnow TE, Rajewsky N (2018) Single-Cell Transcriptomics Characterizes Cell Types in the Subventricular Zone and Uncovers Molecular Defects Impairing Adult Neurogenesis. Cell Rep 25:2457-2469.e2458.